8th March, 2018, University of Brighton, UK

Sergey V. Reznik

THERMOPHYSICAL PROCESSES IN AEROSPACE COMPOSITE STRUCTURES

Department “Rocket and Space Composite Structures”
of the Bauman Moscow State Technical University

E-mail: sreznik@gmail.com

Plan of presentation

Introduction

Features of composite structures

Methodology: modelling and parameter’s identification

Research examples:

- Space antennas
- Reusable space vehicles

Conclusion

Features of composite structures

Composite materials consist of two or more components with a definite interface.

Composites features:

- Characteristics depend on the shape and the manufacturing technology;
- Anisotropy: physical (mechanical, thermal, electrical etc.) characteristics are direction-dependent;
- Stark difference between the matrix and filler characteristics (heat conductivity in CFRP: fiber $\lambda_{\perp} \approx 1$– 5 Вт/(м·К) $\lambda_{\parallel} \approx 20$-300 Вт/(м·К), epoxy resin $\lambda \approx 0{,}25$ Вт/(м·К));
- Laminate structure with an arbitrary number of reinforcement layers;
- Polymer matrix destroyed first under intensive heating

Key requirements for all types composite structures:

- Shape and dimensional stability; high toughness and stiffness; low coefficient of linear thermal expansion;

- Low density (fibrous insulation 60 – 350 kg/m^3, organic polymer 1200-1400 kg/m^3, CFRP 1500-1650 kg/m^3, GFRP 2000-2200 kg/m^3, less than aluminum alloys 2780 kg/m^3, and steel 7800 kg/m^3);

- High thermal resistance 800 К (polymer) – 2500 К (ceramic matrix);

- Long life, reusable?, low maintenance;

- Moderate manufacturing costs.

Methodology: modelling and parameters' identification

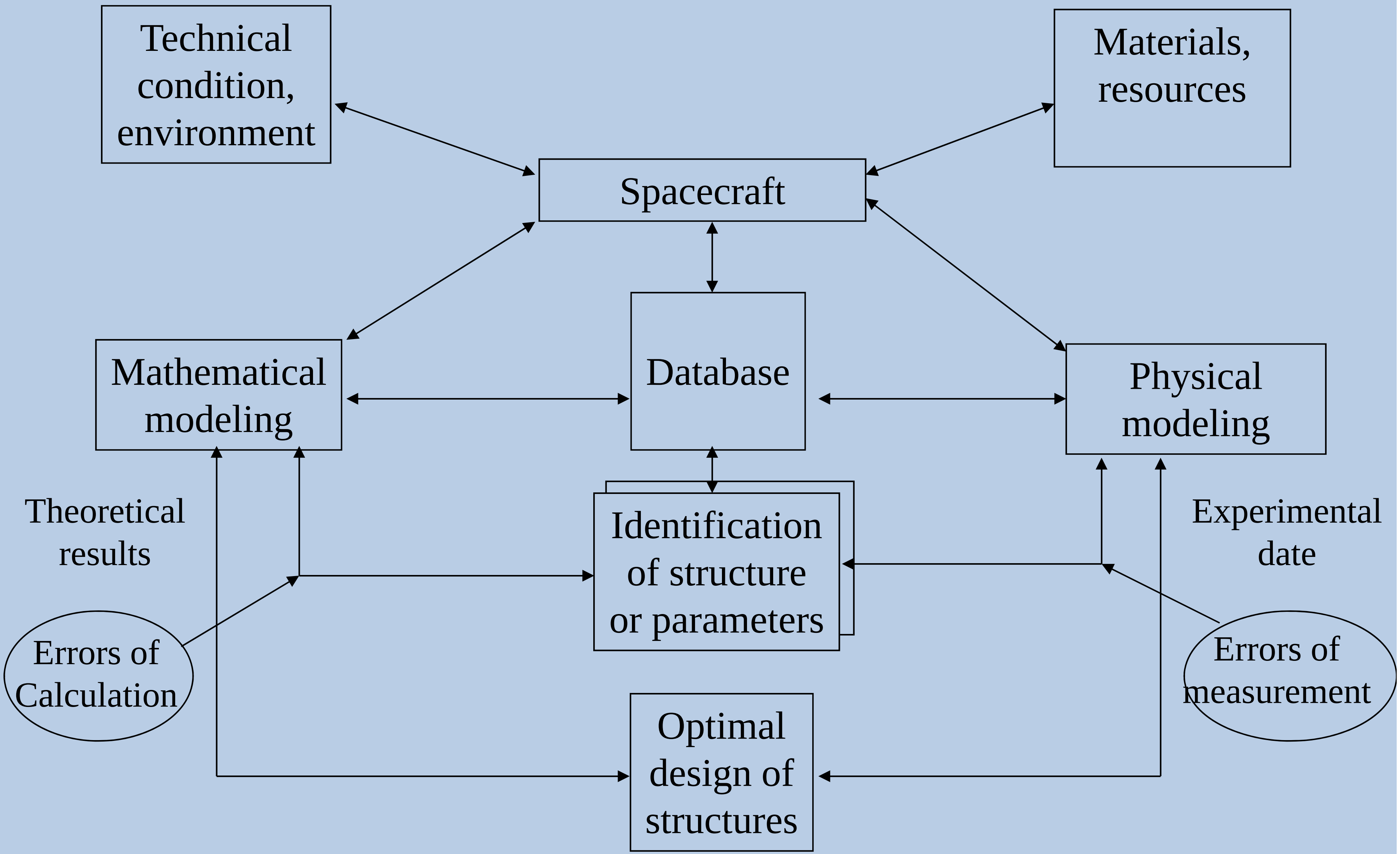

Space antennas

- Short history of space communication
- Modern approaches to reflectors design
- Overview of reflector configurations
- Bauman MSTU space reflector project

Short history of space communication

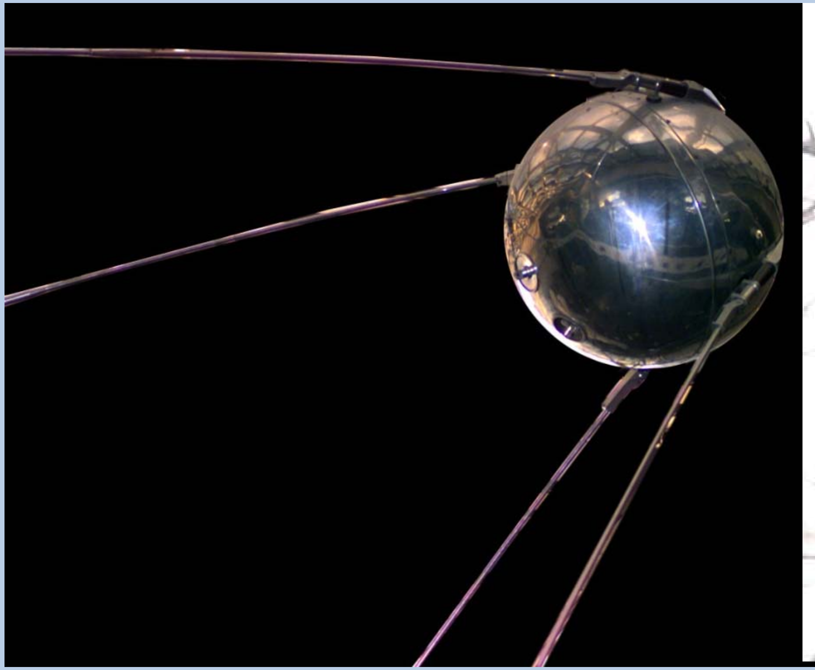

4th October 1957: OKB-1, USSR first artificial satellite "Sputnik"

2 dual-rod omnidirectional rod transmitting antennas l= 2.4 and 2.9 m
ν = 20,005 and 40,002 MHz,
m=83.6 kg, orbit H= 215-939 km; i=65.1°

Short history of space communication

1960's: NASA "Echo" project for transmitting radio waves by satellites looking like a large sphere with thin wall from polymer material and aluminium skin

12.08.1960: "Eho-1" *D*=30.5 m, *m*=76 kg, wall *h*=12.7 mkm, orbit *H*=1520-1687 km; *i*=48°
ν = 960-2390 MHz
25.01.1964: "Eho-2": *D*=41.1 m, *m*=256 kg, wall *h*=17.8 mkm, orbit *H*=1029-1316 km, *i*=81,5°

Short history of space links

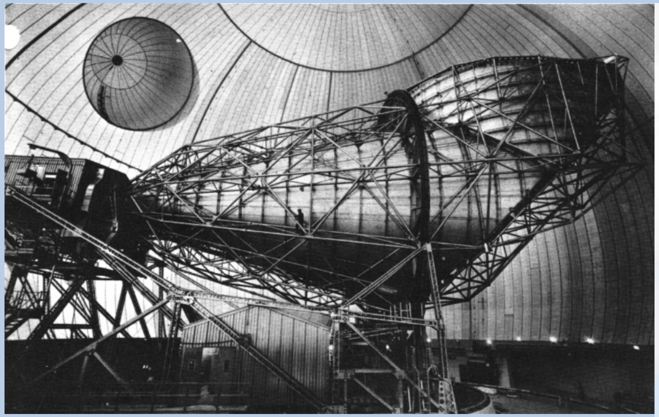

a)

b)

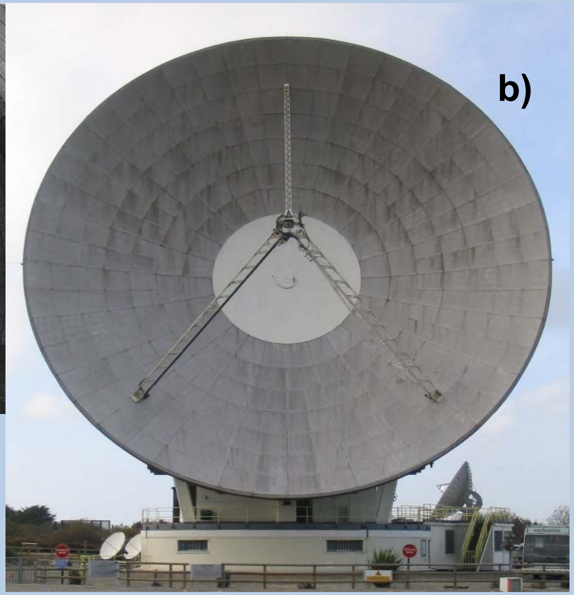

10.07.1962: Bell Telephone Laboratories, USA “Telstar”
An array of antennas around "equator“ of satellite and helical antenna for control commands
ν = 6 GHz (uplink) and 4 GHz (downlink - retransmitting),
***m*=77 kg, orbit *H*= 952-5,632 km; *i*=45°**

a) **The immense horn-reflector antenna within the radome at Andover Earth Station (USA). It consists of a flaring metal horn with a metal reflector mounted in the mouth at a 45° angle. The advantage of this design over a parabolic dish antenna is that it has very low sidelobes; that is, the horn shields the antenna from radiation from angles outside.**

b) **Goonhilly Satellite Earth Station is a large radiocommunication site located on Goonhilly Downs near Helston on the Lizard peninsula in Cornwall, UK. Antenna One (dubbed "Arthur") was the first open parabolic design and is 25.9 m in diameter and weighs 1,118 tonnes.**

Short history of space links

23.04.1965: OKB-1, USSR **"Molniya-1"**
2 umbrella-type reflector antennas *D*=1.4 *m*
ν = 800 MHz (downlink) and 1000 MHz (uplink),
m=1600 kg, orbit *Ha*= 40000 km; *Hp*= 500-2000 km;
i=65.1°

A Soviet-Russian system "**Orbita**" ground antenna for broadcasting and delivering TV signals via "Molniya" satellites

Modern approaches to reflectors design

Shape and size stability under external factors of orbital flight.

Maximum displacement: $<$ 0.3 mm (for 60 GHz antenna)

$\Lambda/16$ (where Λ is the wavelength of the operating frequency of the antenna)

Thermal radiation fluxes from the Sun and the Earth and the associated changes in temperature on the surface of RSA.

The most important stage of the design of RSA is the modelling of temperature and stress-strain state of the composite structure.

The aim of the work is: to select the design layout of ultra-lightweight space antenna reflector from CFRP with high shape and size stability for advanced communication systems

Why carbon fiber reinforced plastic (CFRP)?

- high strength (unidirectional material). 1.3 - 2.1 Gpa ultimate tensile strength;
- high stiffness (unidirectional material): 280-400 GPa tensile modulus ;
- low temperature coefficient of linear expansion of $\pm 0.5 \cdot 10^{-6}$ K^{-1};
- thermal conductivity, within $\lambda_{\perp}$=0,4-0,8 W/(m·K) range;

  $\lambda_{\parallel}$=8-70 W/(m·K) (300 W/(m·K) for pitch-based carbon fibers;
- relatively small density (1500-1650 kg/m^3);
- moderate cost ($1000 per kg);
- a variety of manufacturing methods (infusion, hand layup, winding, etc.)

Geostationary orbit (GEO): relative positions of the Sun, Earth and the satellite orbits

13

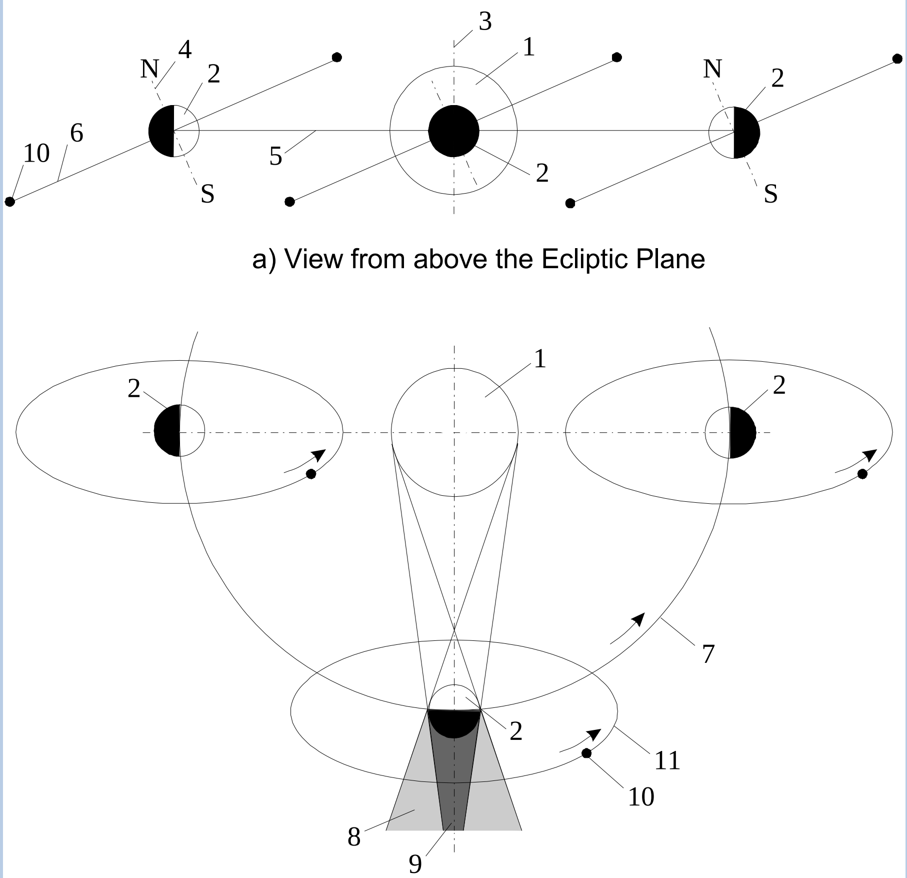

a) View from above the Ecliptic Plane

b) View in the Ecliptic Plane

1 – Sun; 2 – Earth; 3 – Sun rotation axis; 4 – Earth rotation axis; 5 – ecliptic; 6 – Earth equator plane; 7 – Earth orbit; 8 – penumbra; 9 – shadow; 10 – satellite; 11 – satellite orbit

Extreme conditions in geostationary orbit

Height – 35.750 km

Pressure – 10^{-14} mm Hg mm

Temperature – 3 K

Average Sun's heat flux – 1368 W/m^2

Shadow zone 2 times a year during autumn and spring equinox with a total duration of 45 days with a maximum time in the shade of 31 min (LEO) and 71 min (GEO)

Corpuscular radiation:
- the flow of electrons with energy of 0.1 to 4.0 MeV 108 $e^{–}/cm^{2}\cdot c$
- the dose of ionizing radiation of 0.5 rad/day

Operating cycle in space 10-15 years

Overview of the reflectors for space antennas

Sandwich configuration

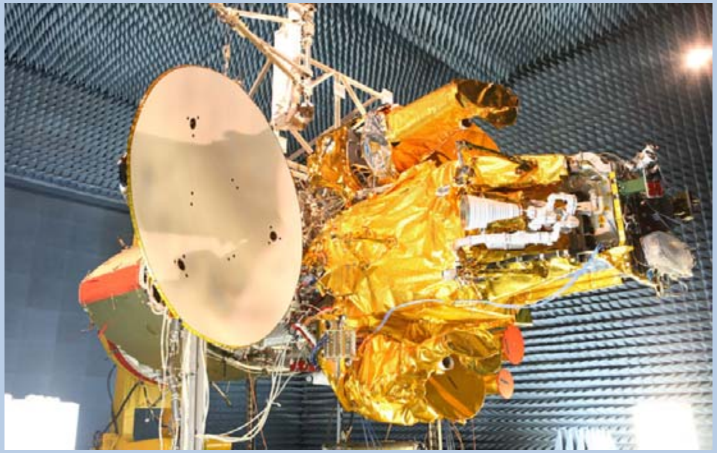

Express-AM33, JSC "ISS n.a. M.F. Reshetnev, and Thales Alenia Space

RUAG Space

Eutelsat 115 West B, Boeing

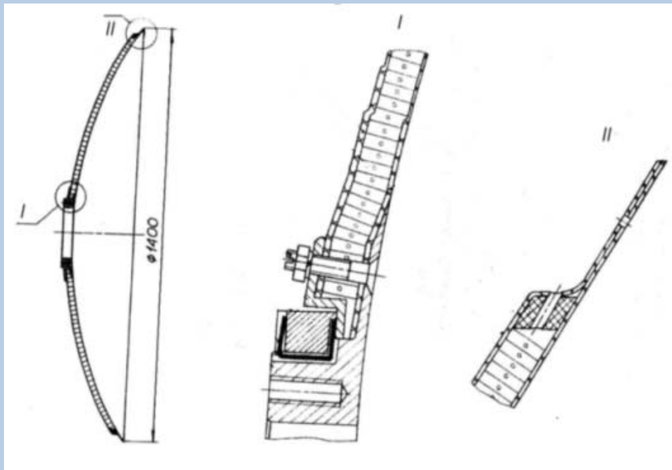

Sandwich structure with a honeycomb core

Overview of the space antennas reflectors:
The truss reinforcement of the convex surface

Yamal-402, JSC "ISS n.a. M.F. Reshetnev, and Thales Alenia Space

Intelsat-36 Space System Loral

Telstar-11 Space System Loral

Overview of the space antennas reflectors:
The ribs reinforcement of the convex surface

Vanguard Space Technologies», USA, dual shell and ribs

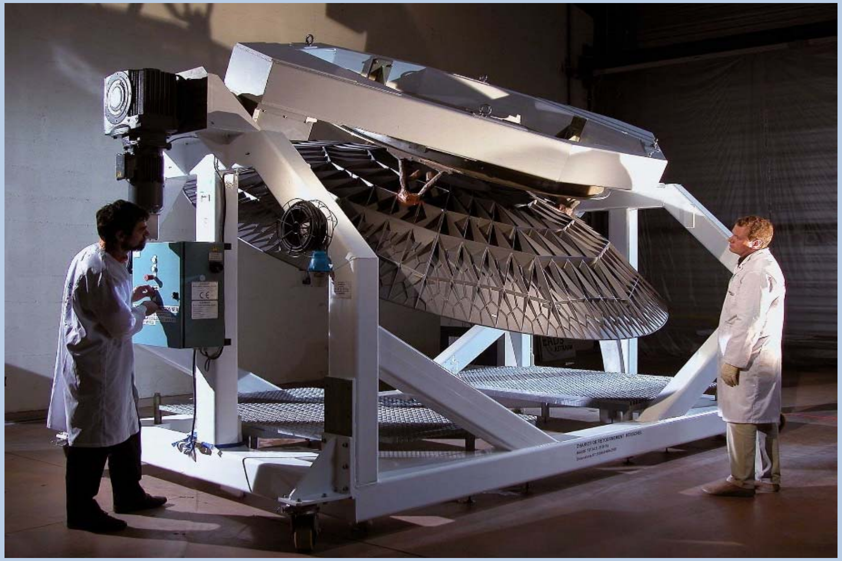

Herschel telescope primary mirror, EADS Astrium

Reflector for Artemis, Alenia Spazio

Overview of the space antennas reflectors:

The ribs reinforcement of the convex surface

Central part of the Astron reflector, JSC "Plastic", Syzran

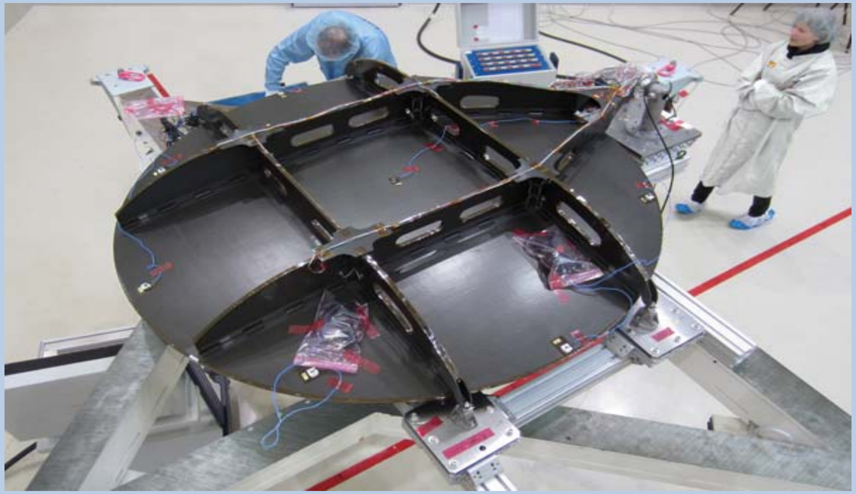

HPS GMbH

Experimental space antenna reflector, JSC "Plastic", Syzran

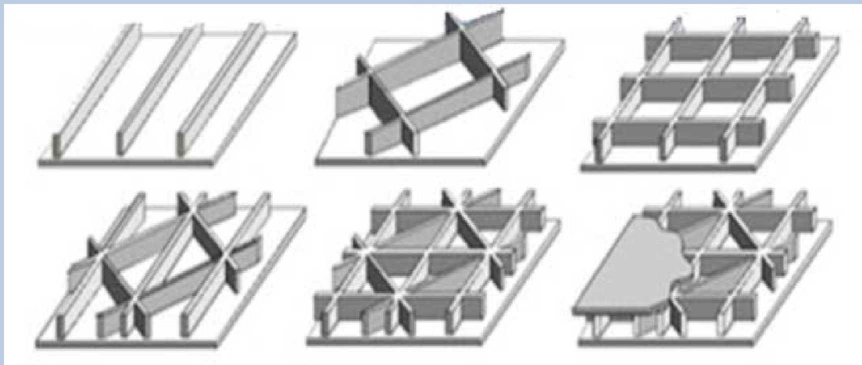

Options ribbed surfaces

Bauman MSTU experience in space antenna reflectors design

The ribs reinforcement of the convex surface

Bauman MSTU reflector with ribbed surface, 2013

Shell thickness, mm	1.0
Weigh, kg	2.08
Aperture diameter, mm	950
Construction height, mm	46.7
Linear mass kg/m^2	2.93
Maximum displacement, mm	0.30

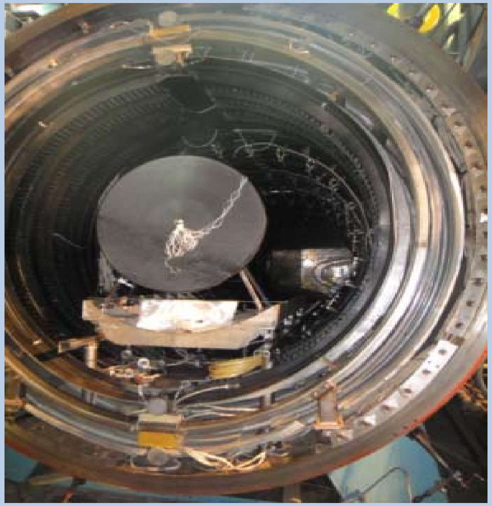

Rational uses of various types of space antenna reflectors

(data by ESA, ESTEC)

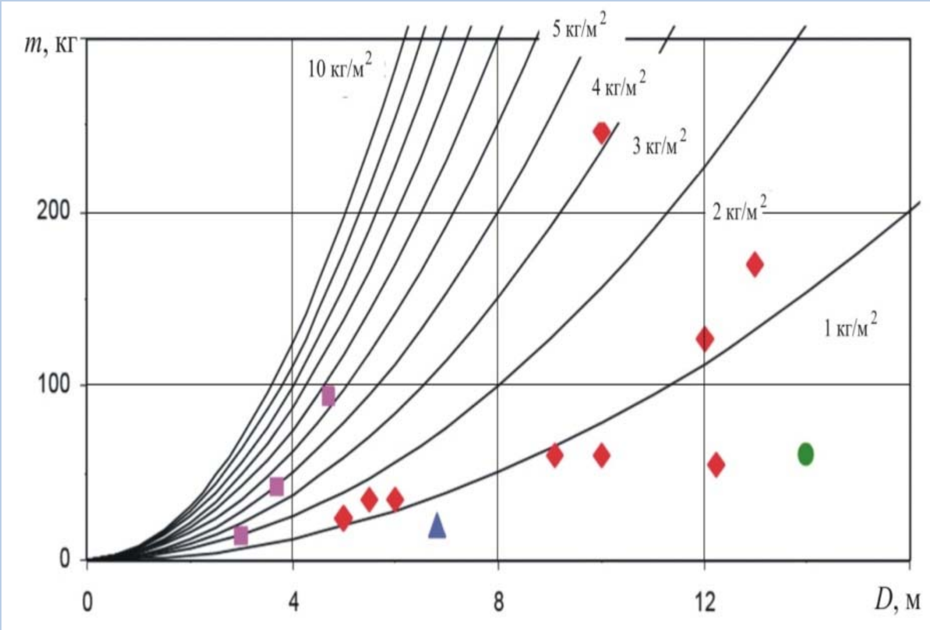

Dependence of reflectors' mass on the diameter:

◆– mesh; ■ – with rigid surface;
● – inflatable; ▲ – with adjustable surface

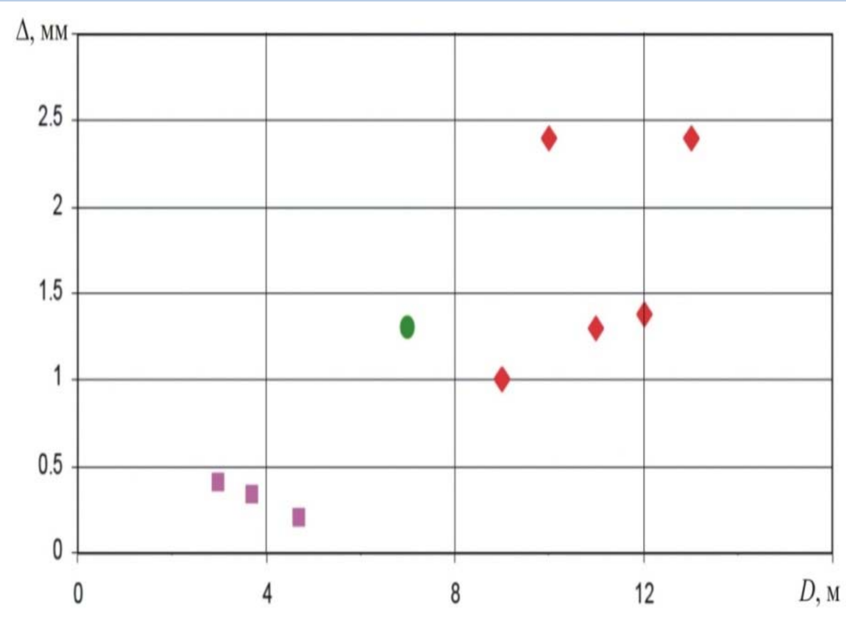

Dependence of reflectors' accuracy on the diameter:

◆– mesh; ■ – with rigid surface
● – inflatable

Design requirements for the advanced space antenna reflector

1. Accuracy of reflector surface (root-mean-square error less than $\Lambda/16$, Λ is wavelength. Displacement 0.1 mm.
2. Strength and stability during spacecraft launch period.
3. High dynamic characteristics (high frequencies of structures, not less than 100 Hz).
4. Operating cycle in space $>$ 15 years.
5. Linear mass of the reflector assembly not greater than 2 kg/m^2.
6. The diameter of the reflecting surface of 1200 mm, focal length 500 mm construction height 180 mm.

Design procedure

- Select one design layout
- Define the thermal loads on the reflector in GEO
- Create the geometric and finite element model of the reflector
- FE modeling of the thermal state using "Siemens Space System Analysis"
- Decide how the reflector will be fixed to the spacecraft
- FE modeling of the stress-strain state using "Siemens NX Nastran"
- Determine the maximum thermal deformation and displacement of the reflecting surface
- Analyze the results and compare with other options design layout variants.

Thermo physical properties of materials

Material	Thermal conductivity, W/(m·K)	Heat capacity, J/(kg·K)	Temperature coefficient of linear expansion, K^{-1}
CFRP	31	1000	$5.27 \cdot 10^{-7}$
Honeycomb filler (longitudinal)	2,5	963	24.2
Honeycomb filler (transverse)	24	963	24.2
Aluminium	159	963	24.2

Design layout variants of antenna reflector

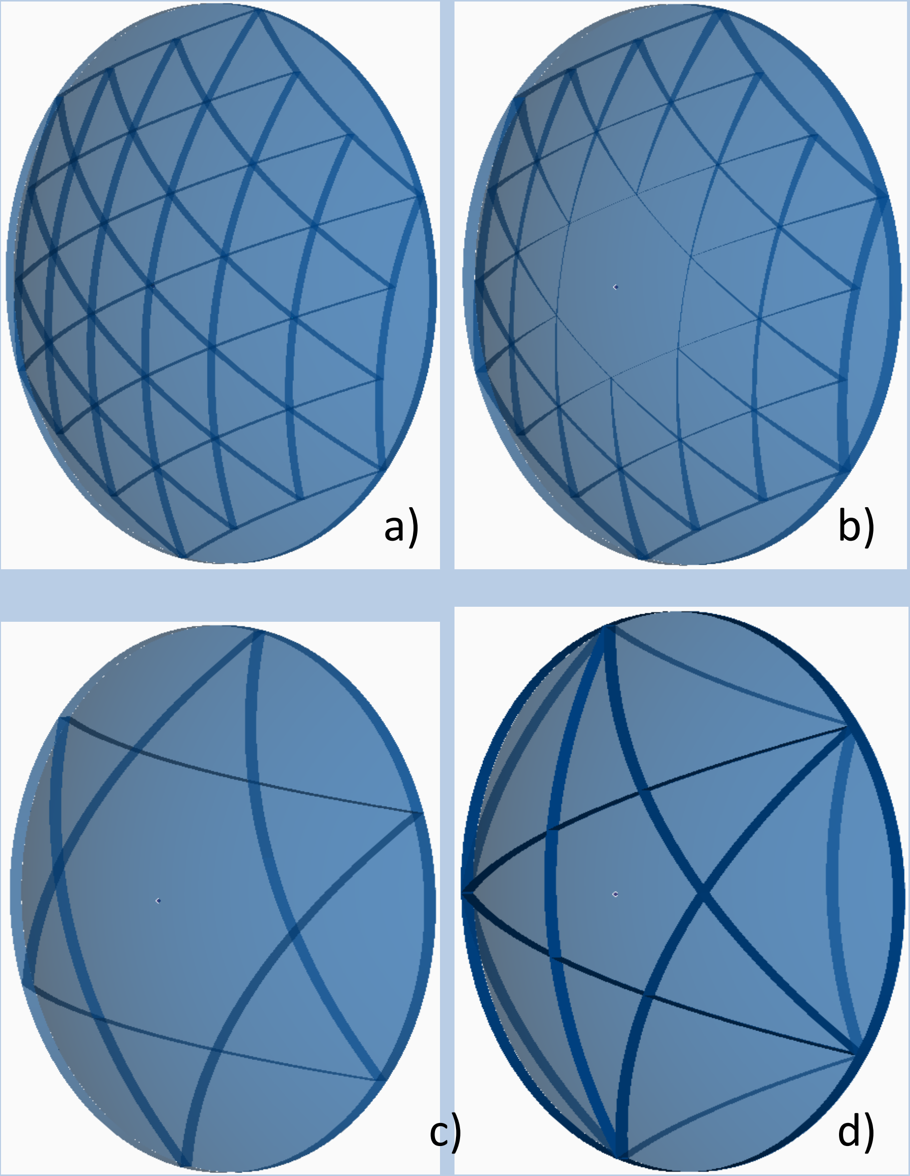

Structure: 6 CFRP layers made of flattened plain weave ASPRO fabric and ED-20 epoxy binder, thickness – 0.4 – 1.2 mm.

Layers orientation: ±90º/ ±90º/ ±90º.

Variants of ribbed reflectors:

a) izogrid with permanent height of ribs;

b) izogrid with variable height of ribs;

c) six pointed star;

d) five pointed star

Parameters of layouts for numerical modeling

Name of variant	Ribbed scheme	Height of ribs, mm	Thickness of ribs, mm	Thickness of shell, mm
Star6_25_12_06	Six pointed star	25	1,2	0,6
Star6_60_06_06	Six pointed star	60	0,6	0,6
Star6_90_06_04	Six pointed star	90	0,6	0,4
Star5_90_06_04	Five pointed star	90	0,6	0,4
Star5_53_06_06	Five pointed star	53	0,6	0,6

Thermal state numerical modeling

for six-pointed star

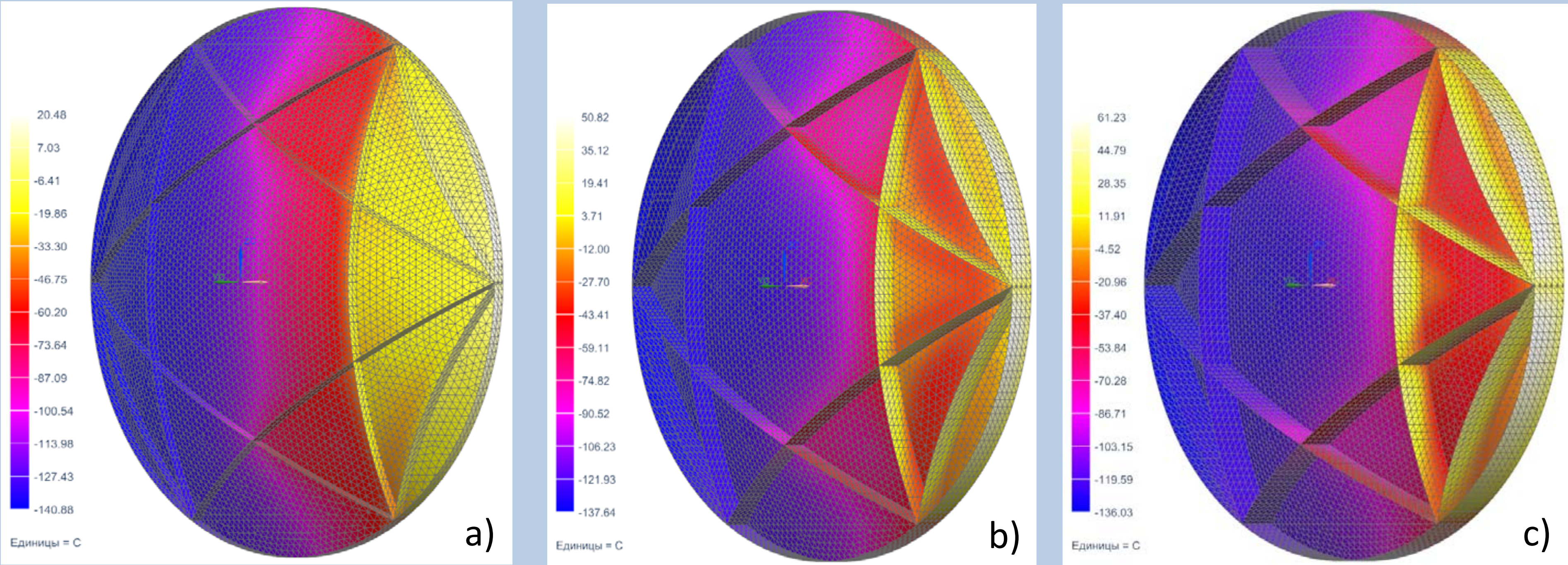

Temperature state of the reflector (degrees Celsius) for:

a) Star6_25_12_06, b) Star6_60_06_06, c) Star6_90_06_04

with 270º angle between reflector rotation axis and the Sun – Earth line

Temperature state numerical modeling for five-pointed star

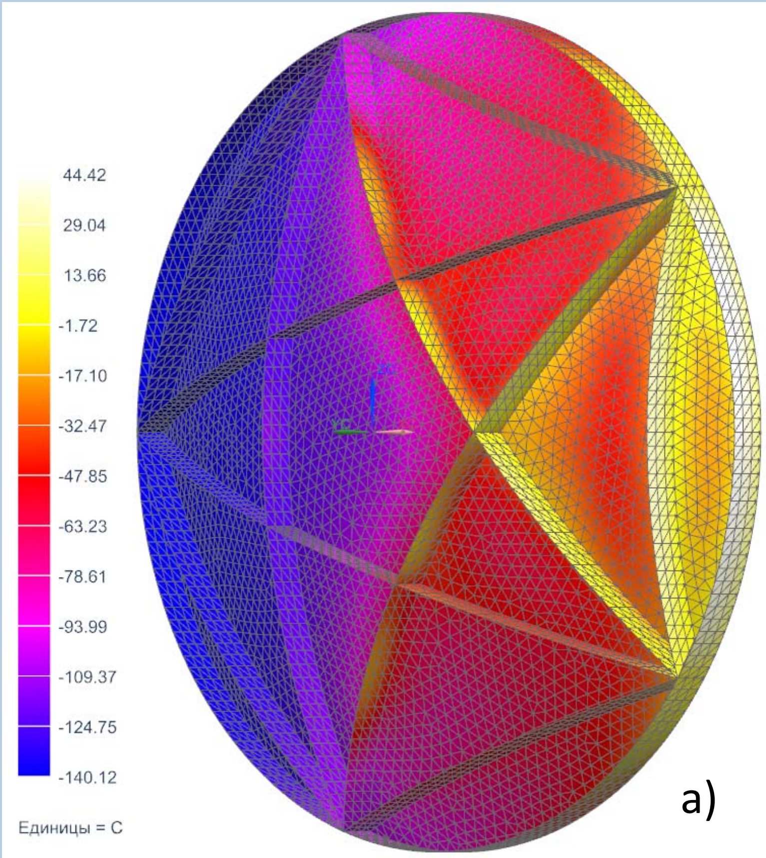

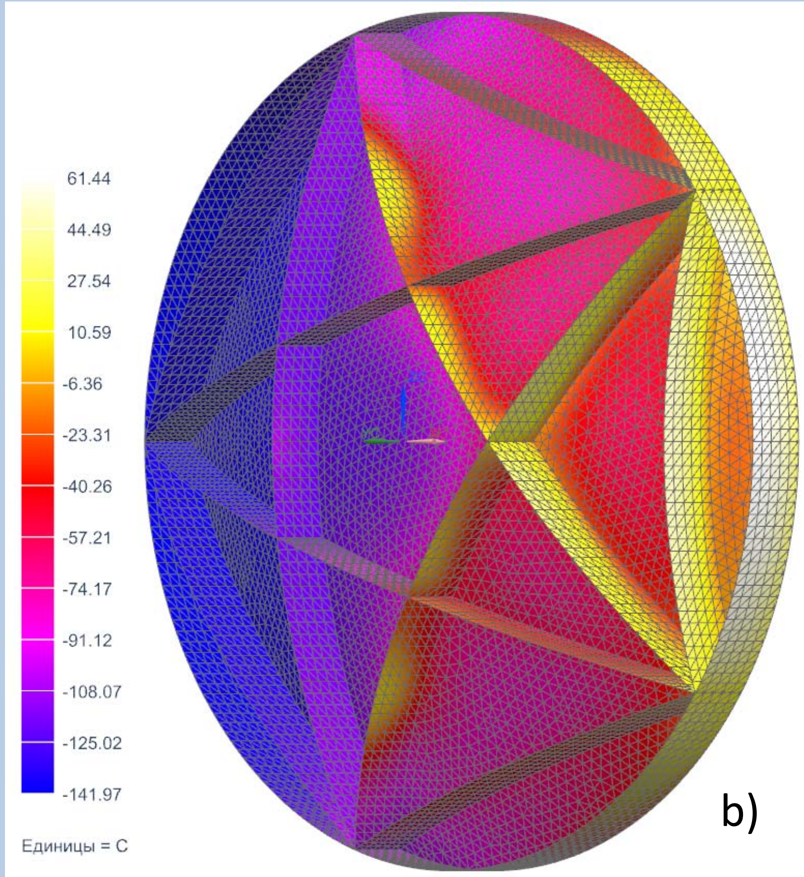

Temperature state of the reflector (degrees Celsius) for:
a) Star5_53_06_06, b) Star5_90_06_04
with 270º angle between reflector rotation axis and the Sun – Earth line

Comparison of ribbed design layouts

Scheme of ribbed surfaces	Shell and ribs thickness, mm	Mass of the reflector, kg	Maximum displacement of reflecting surface, mm	Linear density, kg/m^2
Six pointed star	0.6	1.523	0.14	1.354
Five pointed star	0.6	1.502	0.12	1.328
Izogrid with permanent height of ribs	0.6	1.549	0.185	1.369
Izogrid with variable height of ribs	0.6	1.479	0.18	1.308

Stress-strain state for six-pointed star

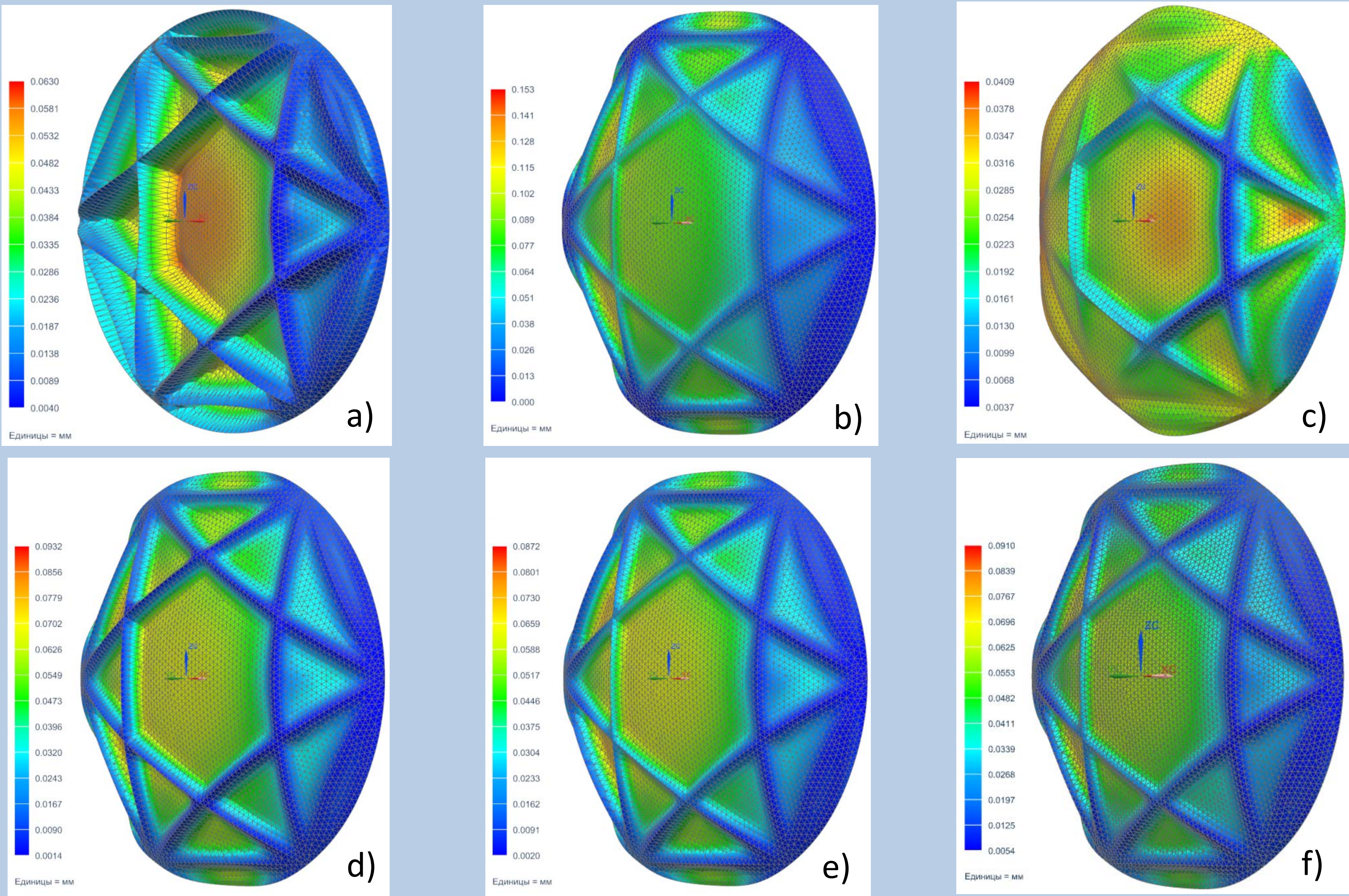

Displacement of reflecting surface (mm) under the action of thermal loads for Star6_90_06_04
a) circular; b) prop; c) center; d) beams; e) frame; f) assemblies (nodes)

Stress-strain state for five-pointed star

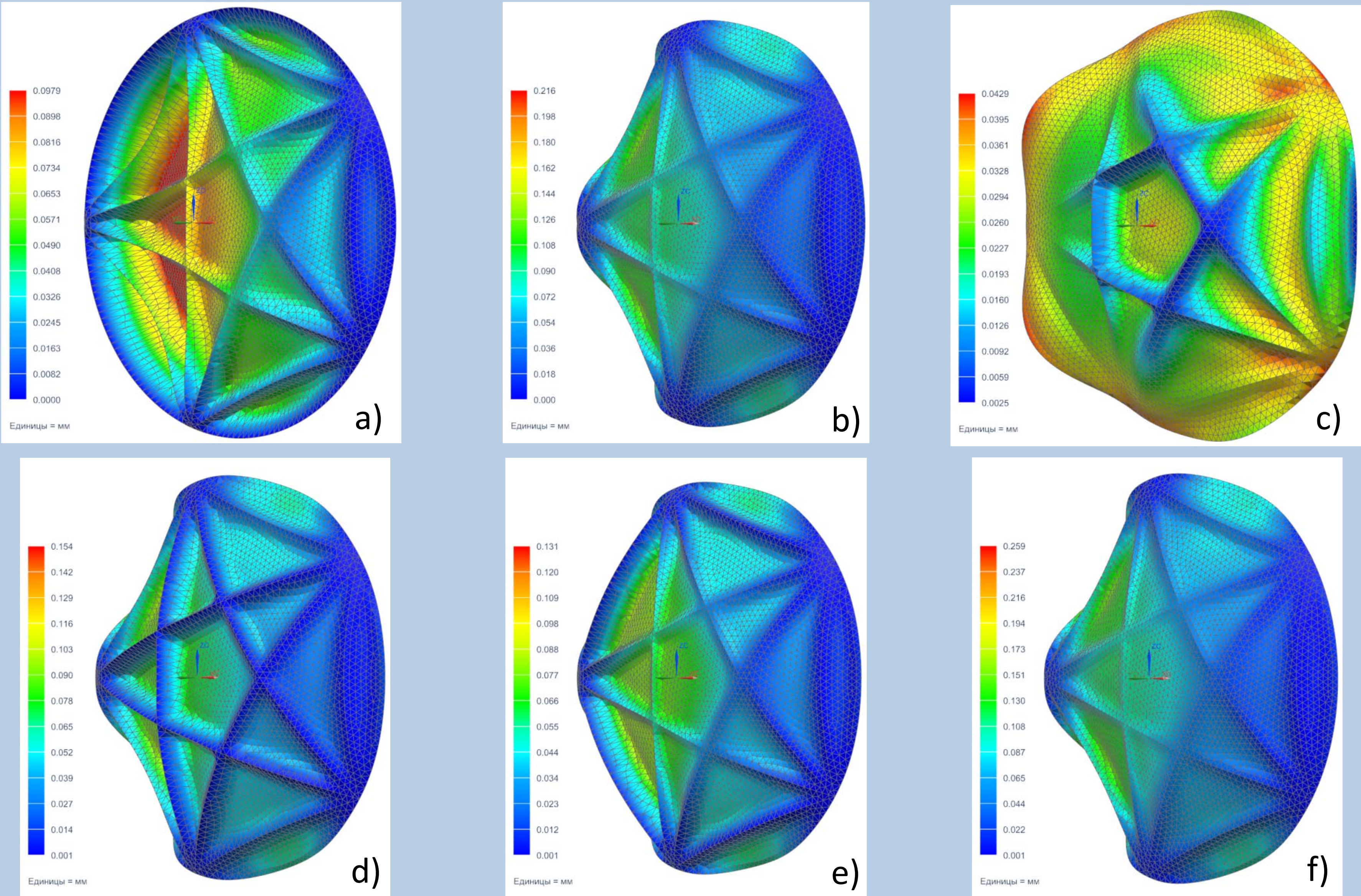

Displacement of reflecting surface (mm) under the action of thermal loads for Star5_53_06_06:
a) circular; b) prop; c) center; d) beams; e) frame; f) assemblies (nodes)

30

Comparison of reflector design layout

Design layout	Displacement of reflecting surface under the thermal loads, mm	Linear density, kg/m^2
Sandwich	0.238	2.3
Double shell	0.047	3.5
Ribbed shell “six pointed star”	0.041	1.6

Bauman MSTU space antenna reflector - 2016

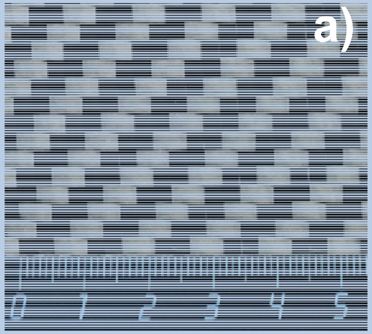

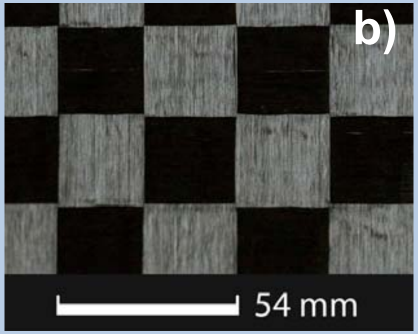

The thickness of the shell, mm	0.6
Weigh, kg	2.50
Aperture diameter, mm	1200
Construction height, mm	180
Linear density kg/m^2	1.92
Maximum displacement, mm	0.04

2-D Durable fabric based on:
a) conventional tow; b) flattened tow

Conclusion-1

1. Several reflector design options with ribbed convex surface were analyzed, showing the superiority of the six pointed star pattern, thin-walled shell configuration

2. Simulation of temperature and stress-strain state showed that for the GEO, the maximum temperature differences can be up to 220° C, and the maximum displacement will not exceed 0.041 mm.

3. Comparison with the conventional configuration (honeycomb and double shell) showed a significant (up to 2 times) reduction in the linear density of the structure combined with the best shape and size stability.

Reusable space vehicles

- New generation of reusable space vehicle
- Features of reusable thermal protection systems
- Structure of insulation material and mathematical models
- Methodology of theoretical and experimental investigation
- Results. Comparison and analysis

Importance of the problem

• The materials with low density, low heat conductivity, high thermal stability, available in technological attitude and inexpensive are preferred for thermal protective system (TPS) of reusable space vehicles (RSV).

• The create TPS with optimum weight-geometric and economic characteristics it is topical to determine with a required degree of accuracy thermo-physical properties of porous materials for operating conditions.

The aim of the work is: investigation of combined heat transfer regularities in porous thermal protective materials for RSV at wide temperatures interval (300-2000 K) and at high rates of heating (up to 100 K/s).

New generation of reusable space vehicle

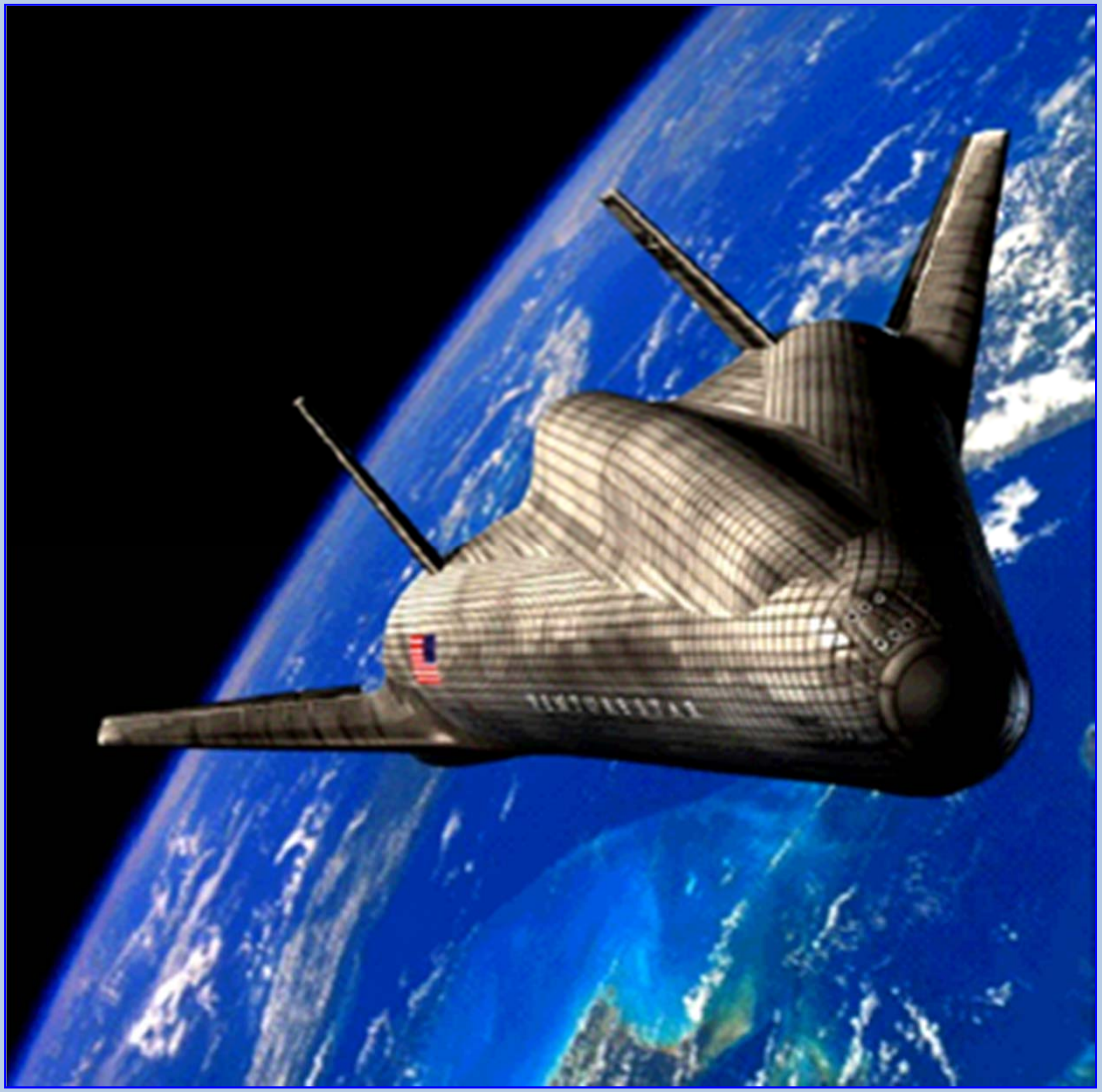

One-stage Reusable Launch Vehicle *Venture Star*, Designed by Lockheed Martin

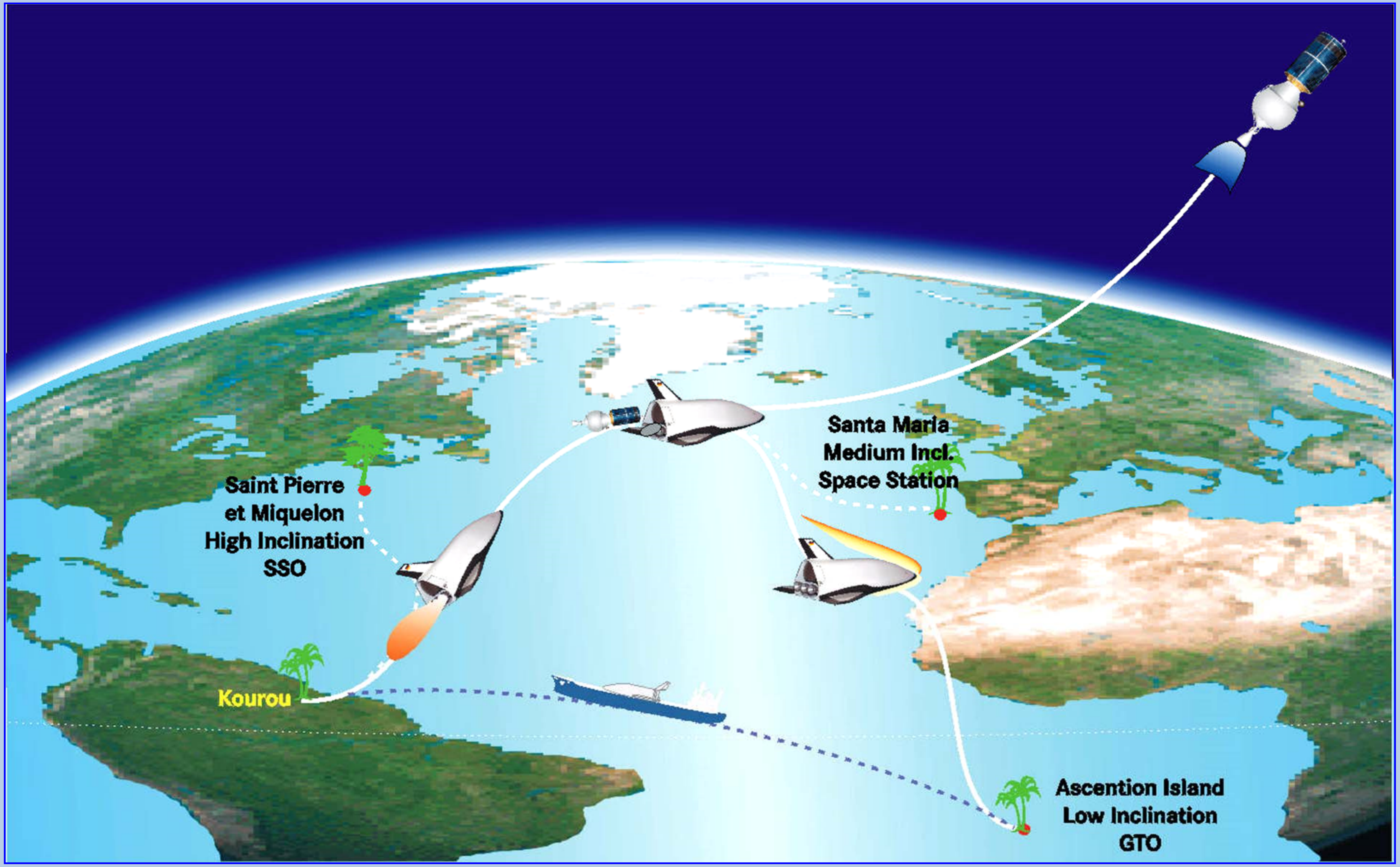

One-stage Reusable Launch Vehicle *Hopper*, Designed by EADS Company

One-stage Reusable Launch Vehicle *Sivka*,
Designed in the Frame of Education Process at Bauman MSTU

**Mock-up of the Orbital Reusable Launch Vehicle *Cliper*,
Designed in Korolev Rocket Space Corporation**

Features of reusable thermal protection systems

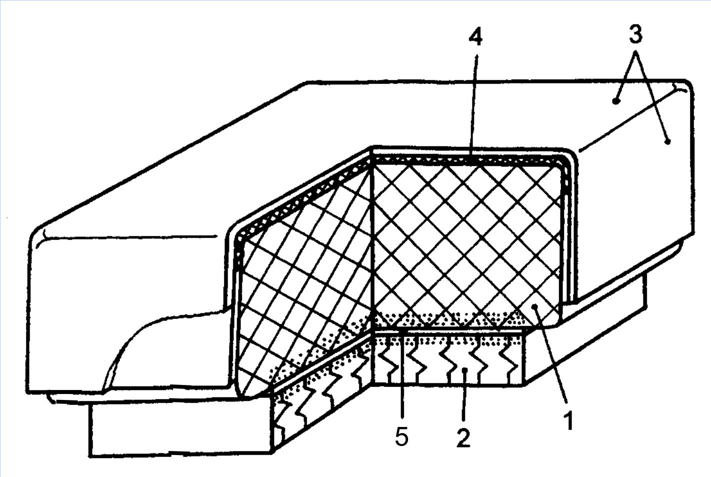

a

a – Space Shuttle, Buran; *1* – tile from sintered silica (quartz fiber insulation); *2* – tense felt compensator; *3* – varnish; *4* – vitreous coating (borosilicate glass); *5* – hermetic glue;

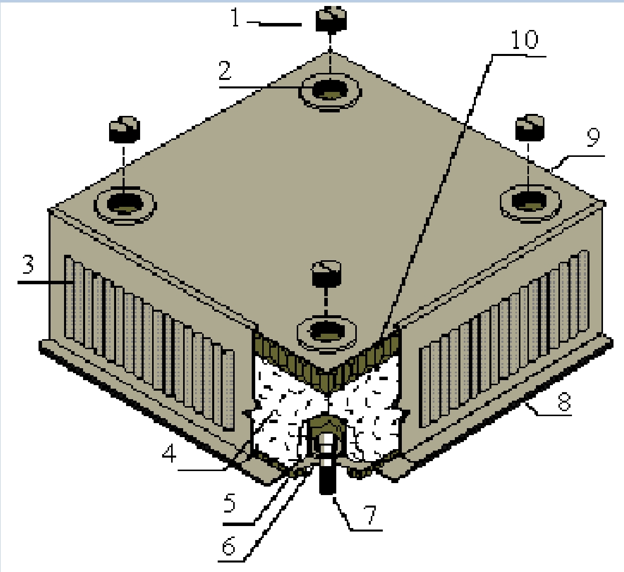

б

b – Advanced reusable launch vehicle;
1 – fastener access cover; 2 – fastener access tube;
3 – beaded Inconel side closure; 4 – saffil alumina insulation; 5 – titanium honeycomb;
6 – titanium foil; 7 – mechanical fastener;
8 – underhanging lip; 9 – overhanging lip;
10 – inconel honeycomb sandwich.

Structure of insulation material and mathematical models

Structures

Opaque materials

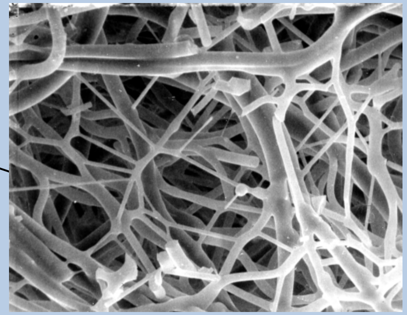

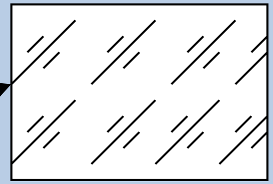

Semitransparent material

Mathematical models

Model of effective thermal conductivity (ETC)

λ_{eff} - effective thermal conductivity coefficient;
C - volumetric capacity;
ε - emissivity.

Model of radiative and conductive heat transfer (RCHT)

Parameters

λ - molecular coefficient of thermal conductivity;
C - volumetric capacity;
α - absorption coefficient;
β - scattering coefficient;
ω - albedo;
$\rho(\lambda)$ - scattering indicatrix;
ε - emissivity in opaque range of specter

Open questions:

- What are the conditions (type of heating regimes, time of testing, properties of materials, etc) when the role of radiative heat transfer in materials can be neglected in a wide range of temperatures?

- What is the temperature dependence of effective thermal conductivity coefficient $\lambda_{ef}\,(T)$ of porous materials in a wide range of heating velocity?

Methodology of theoretical and experimental investigation

• Mathematical simulation and designing of thermal test conditions.

• Thermal tests of samples of new porous materials and measurements of temperature distribution inside samples.

• Heating methods – contact, radiative or convective.

• Solution of a 1-D and 2-D inverse problems of effective thermal conductivity (ETC) and radiative and conductive heat transfer (RCHT).

Experimental equipment

Table 1. Characteristics of thermal test equipment

Characteristic	Title, owner				
	«Uran-1», HMTI n.a. A.V. Luikov, Minsk, Belarus	«Luch-2», HMTI n.a. A.V. Luikov, Minsk, Belarus	T-52A, CAHI n.a. N.E. Zhukovskiy, Moscow region, Russia	Solar concentrator, PSA, Tabernas, Spain	TC-3000, ARIAM, Moscow, Russia
Heating type	Concentrated plasma radiation	Combined (radiation and convection)	Contact	Concentrated solar radiation	Flash laser radiation
Maximum sample dimension (length × width × hight or diameter × length), mm	∅ 60 × 20	∅ 14 × 150	152 × 152 × 50	∅ 230 × 500	∅ 10 × 2.5
The capacity, kW	up to 10	450	up to 10	58	up to 3
Maximum heat flux, W/m^2	$0.6 \cdot 10^7$	$1.5 \cdot 10^7$	$5 \cdot 10^6$	$3.0 \cdot 10^6$	$3.5 \cdot 10^7$
Heat flux inequality, %	15 %	15 %	1 %	5 % (∅ 230 mm)	1 %
Maximum testing time, minutes	10	10	up to 600	300	up to 0.3
The testing atmosphere, pressure, Pa	air, 10^5	air, 10^5	air, N_2, Ar, vacuum, $1 - 10^5$	air, N_2, Ar, vacuum, $10^{-4} - 10^5$	air, N_2, vacuum $1.3 \cdot 10^{-3} - 10^5$
The diagnostic tools	Pyrometer, thermocouples	Pyrometer, thermocouples	Thermocouples radiation heat flux sensors	CCD camera, pyrometer, thermocouples	Thermocouples, pyrometer

Setup of transient experiment

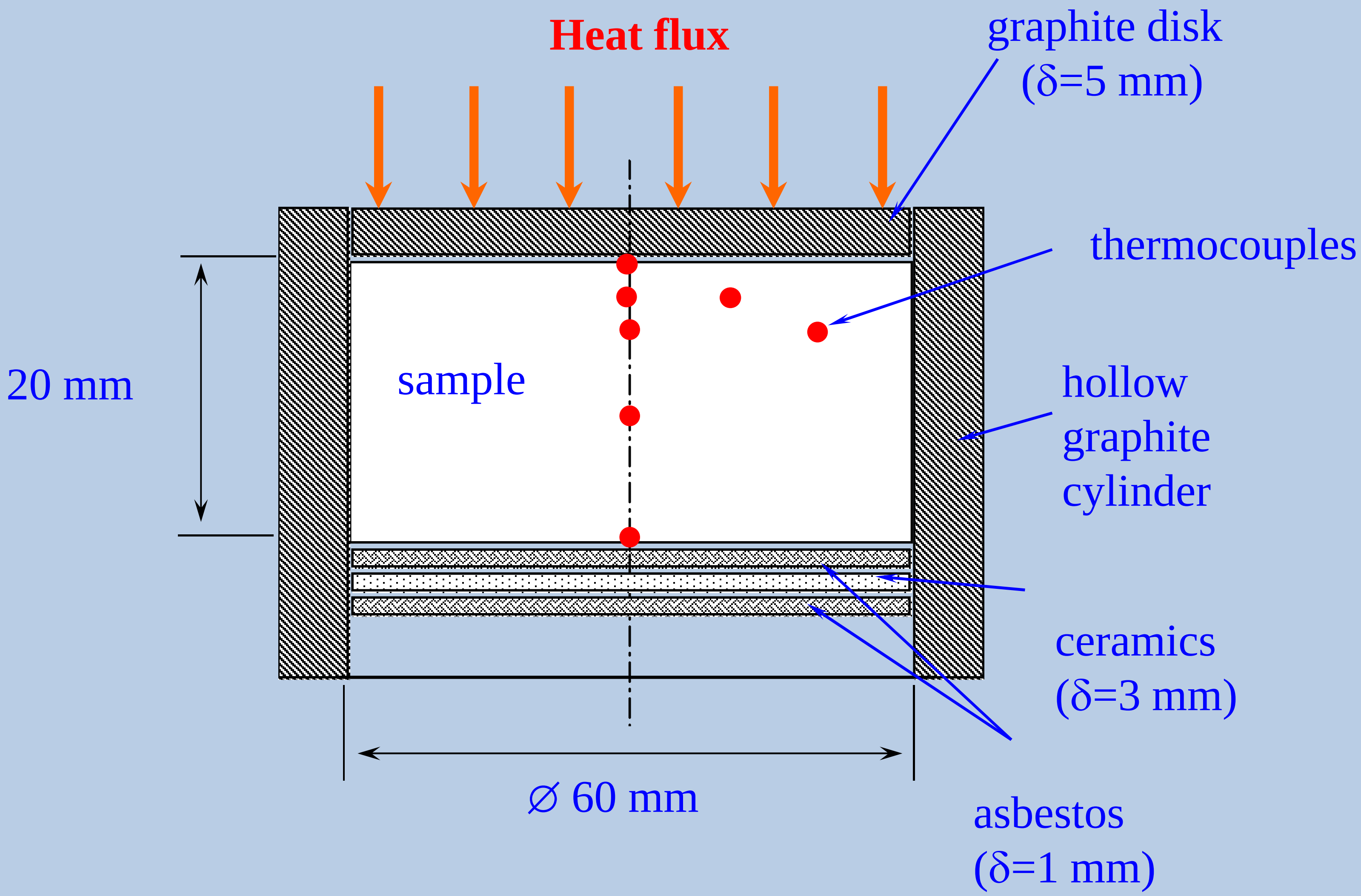

Arc-lamp radiation heater “Uran-1” of HMTI n.a. A.V. Luikov

This installation allows to generate a focused beam with the radiation energy of density up to **$6{\cdot}10^6$ W/m^2** on 12 mm diameter spot

The Plataforma Solar de Almería (PSA) is a center for the exploration of the solar energy, Tabernas, Almeria, Spain

Solar furnace of PSA, Tabernas, Almeria, Spain

Experimental assembly for tests with the solar furnace

Thermal tests on the solar furnace of PSA

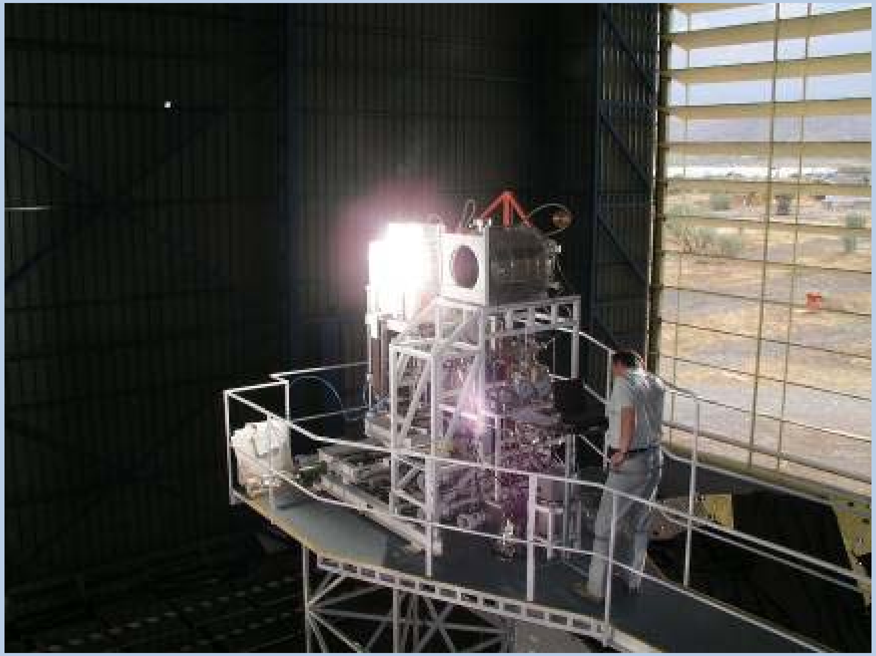

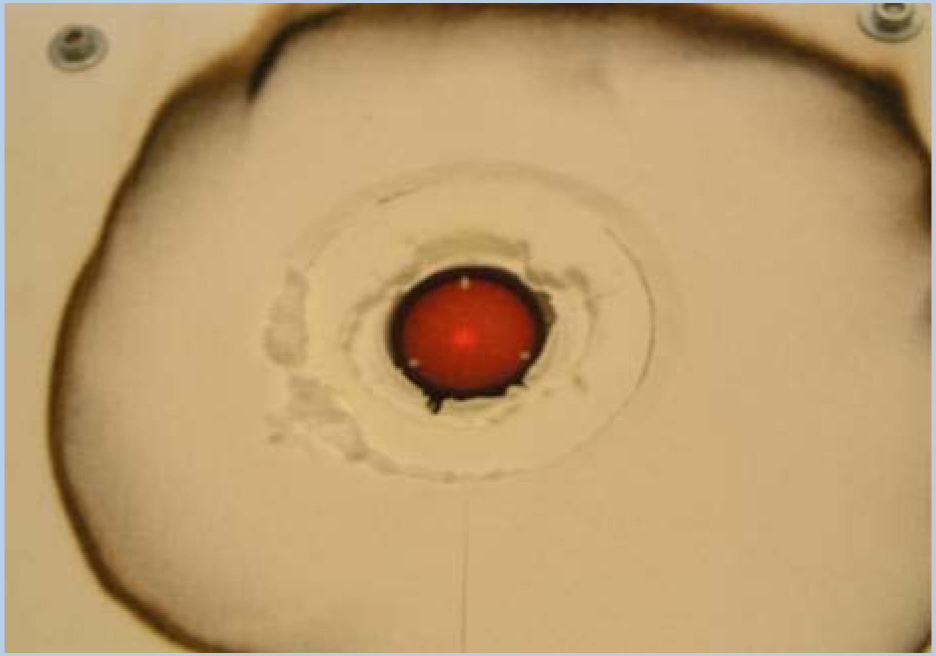

The installation allows to generate a focussed beam with the radiation energy up to **$3 \cdot 10^6$ W/m^2** on 350 mm diameter spot.

Experimental sample – ABS Ceramic on the base Al_2O_3, r = 120 kg/m^2

Experimental conditions: air, $\boldsymbol{T_f}$ = 30 ^oC,

$\boldsymbol{q_{W,R}}$ = 15.0, 37.0, 50.0, 70.0, 120.0, 190.0 · **10^6 W/m^2**

Typical experimental data

CAHI n.a. Zhukovskiy hot guard plate installation

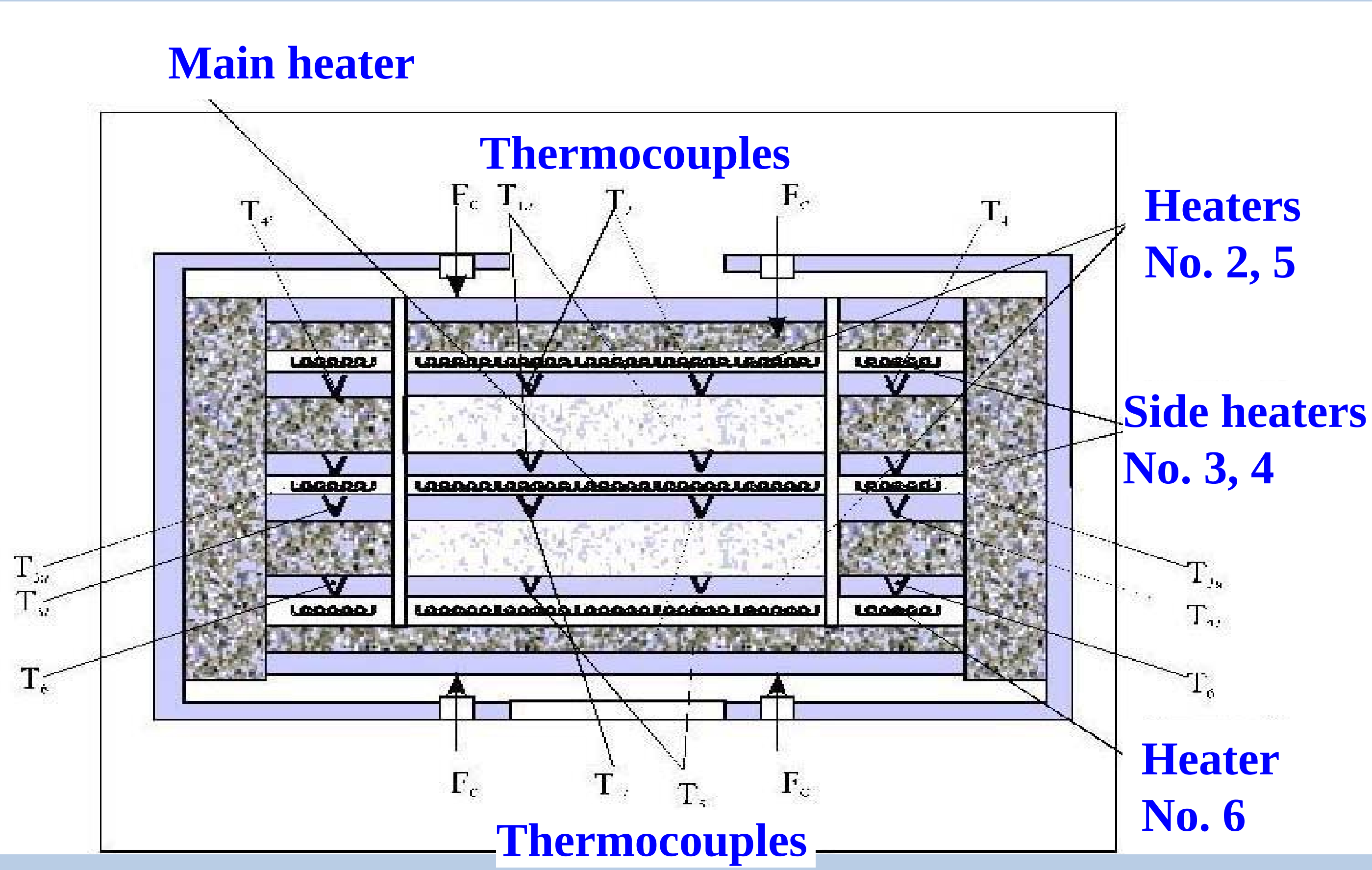

Results. Comparison and analysis

Fibrous SiO_2-based material

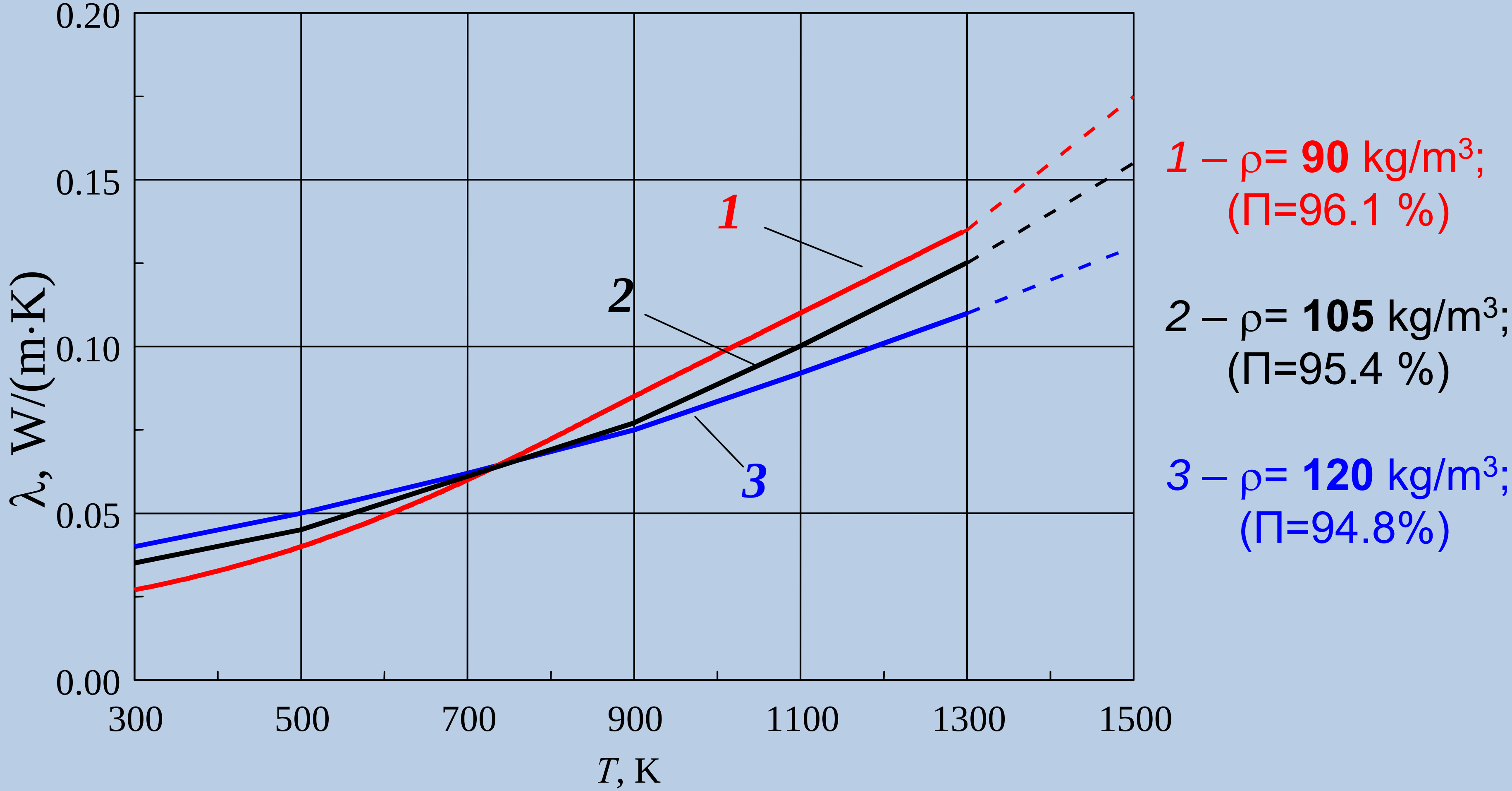

Dependence of effective thermal conductivity on the temperature. Diameter of the fibers is **3 μm**

Comparison with experimental data for stationary conditions
Fibrous SiO_2-based material

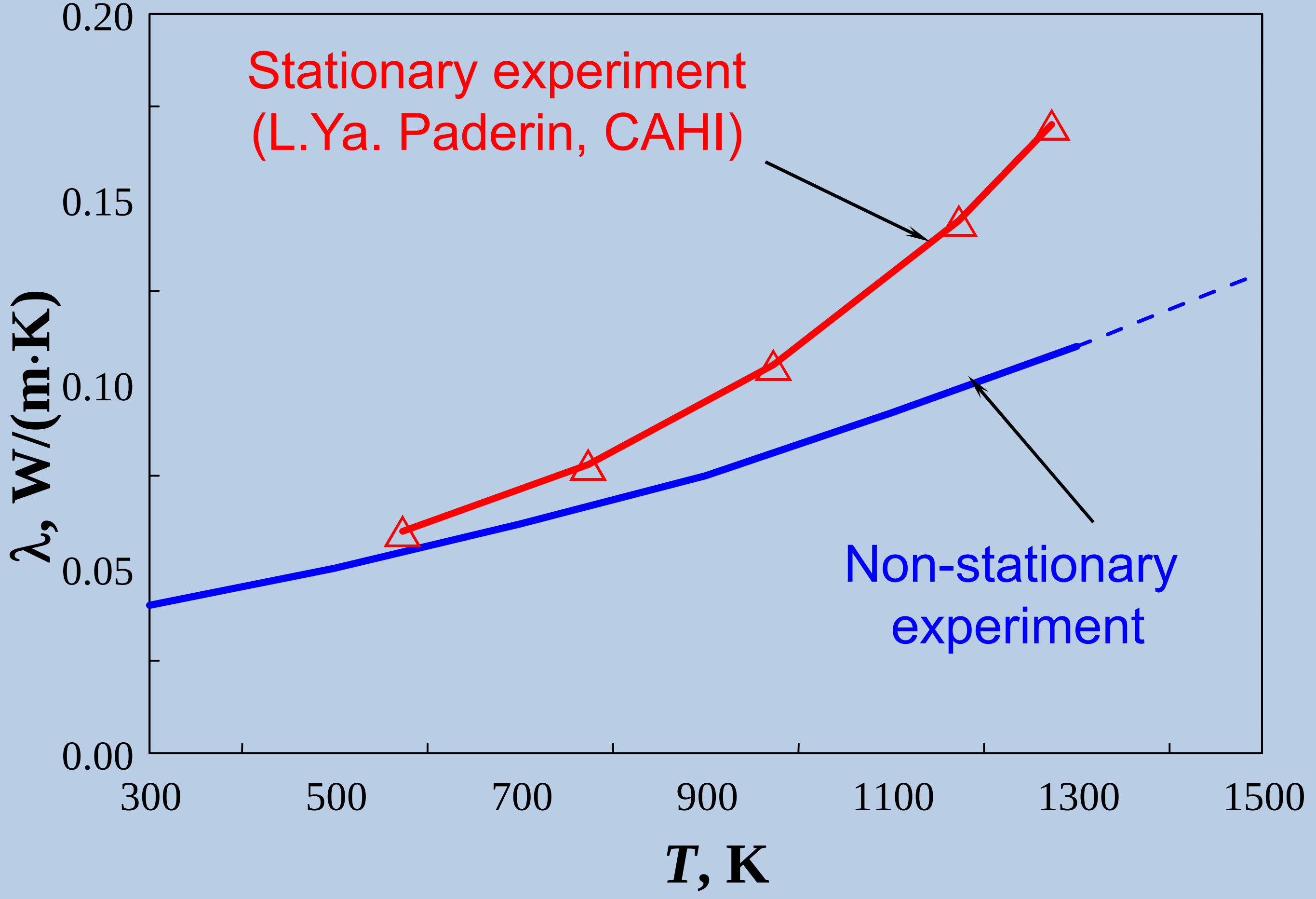

Conclusion-2

1. One of the most important problems in designing reusable launch vehicles is thermal protection system.

2. To create new thermal protection systems it is necessary to account for uncertainty with regard to the type of mathematical models and thermal physical properties.

3. Thermal design is conducted via mathematical modeling and inverse parametric identification. These methods must be employed to predict the thermal stability of systems in case.

Acknowledgement

The author would like to acknowledge

S.A. Gusev, O.V. Denisov, A.D. Novikov, P.V. Prosuntsov

and I.R. Shafikova for their scientific cooperation.

Separate parts of this work are fulfilled with financial support on contract from Russian Ministry of Education and Science on project 14-513-0002-046 and 14.577.21.0023 (Unique identifier of the project RFMEFI57714X0114).

.

Apendix

Software package CAR (Conduction and Radiation)

The package is being worked out at Bauman MSTU since the end of 1970's. It includes FORTRAN-codes for solving direct and inverse problems. The theoretical base of the CAR package approaches are:

•Numerical solving of direct problems (finite difference or finite element methods).

•Extreme statements of inverse problems.

•Parameterization of sought dependencies with splines.

•Iteration regularization method.

•Multi-parameters conjugant gradient method optimization with an additional task in analytical or finite difference form.

•Combined conditions for the cessation of the iteration process of functional minimization (coalescence of sought parameters, minimum generalized discrepancy).

Content of software package CAR

No.	Shape of sample. Material. Statement of IP. First use.	Measurement values / Sought parameters	Features of the method of solving IP
1.	Plate, hollow or utter cylinder. Semitransparent. 1–D IP RHCT for steady state conditions. Since 1984	Heat flux and temperatures on the both surfaces of sample / Coefficient of molecular (pure) thermal conductivity λ	Finite-difference method of solving the direct problem. One-parameter method optimization (DSC-Powell's method).
2.	Plate. Semitransparent. 1–D IP of RHCT for regular conditions. Since 1984	Temperatures on the both surfaces and in the centre of the sample / Coefficient of molecular (pure) thermal conductivity $\lambda (T)$.	Same as in point 1
3.	Plate, hollow or utter cylinder. Semitransparent or opaque. 1–D IP RHCT or IP ETC for transient conditions. Since 1984	Temperatures in several points inside the sample or in one point in the sample and heat flux on one of its surfaces / Simultaneously coefficient of molecular thermal conductivity $\lambda (T)$ or effective $\lambda_{ef} (T)$, and volumetric heat capacity $C (T)$.	Finite difference method of solving the direct problem. Multi-parameters conjugant gradient method optimization with an additional task in finite difference form.

Content of software package CAR

No.	Shape of sample. Material. Statement of IP. First use.	Measurement values / Sought parameters	Features of the method of solving IP
4.	Plate. Semitransparent. 1–D IP of radiation transfer. Since 1984	Spectral transmission or reflectivity of a few samples with different thickness / Simultaneously spectral coefficient of absorption k_ν and coefficient of scattering β_ν.	Finite difference method of solving the direct problem. Two-parameters optimization for each point of spectrum.
5.	Plate. Opaque, orthotropic. 2–D IP ETC for transient conditions. Since 1988	Temperatures in a several points inside the sample or in two points in the sample and heat flux on one of its surfaces / Simultaneously coefficients of heat conductivity $\lambda_x (T)$, $\lambda_y (T)$, and volumetric heat capacity $C (T)$.	Finite difference method of solving the direct problem. Multi-parameters conjugant gradient method optimization with additional task in finite difference form.
6.	Rectangular rod. Opaque, orthotropic. 2–D IP ETC for steady state conditions. Since 1990	Temperatures in three points of the sample (in the middle of two nearby surfaces and on the verge of sample / Simultaneously coefficients of heat conductivity λ_x, λ_y, and emissivity ε.	Finite element method of solving the direct problem. Improved simplex method optimization (Nelder-Mead's method**).**

Content of software package CAR

No.	Shape of sample. Material. Statement of IP. First use.	Measurement values / Sought parameters	Features of the method of solving IP
7.	Plate. Semitransparent or opaque, orthotropic. 2–D IP RCHT or ETC for transient conditions. Since 2003	Temperatures in several points inside the sample or in two points in the sample and heat flux on one of its surfaces / Simultaneously coefficient of molecular thermal conductivity $\lambda_x (T)$, $\lambda_y (T)$ or effective $\lambda_{x\ ef} (T)$, $\lambda_{y\ ef} (T)$, and volumetric heat capacity $C (T)$.	Finite element method of solving the direct problem. Multi-parameters conjugant gradient method optimization with an additional task in analytical form. Vector method for the choice minimization steps.
8.	Plate, hollow or solid cylinder. Semitransparent. 1–D IP RCHT for transient conditions. Since 2005	Temperatures in a few point inside sample or in one point in the sample and heat flux on the one surface / Simultaneously coefficient of molecular thermal conductivity $\lambda (T)$, volumetric heat capacity $C (T)$, coefficient of absorption $k(T)$, and coefficient of scattering $\beta(T)$.	Finite element method of solving the direct problem. Multi-parameters conjugant gradient method optimization with additional task in analytical form. Vector s method for the choice minimization steps.
9	Plate, opaque. 1–D IP ETC for transient conditions after laser flash. Since 2005	Temperatures on a back side of sample / Simultaneously coefficient of thermal conductivity λ, volumetric heat capacity C.	Finite difference method of solving the direct problem. Multi-parameters conjugant gradient method optimization with an additional task in analytical form. Vector’s method for choice minimization steps.

New Approaches in Inverse Problem Solutions

Statement of 2-D Inverse Problem of Radiative and Conductive Heat Transfer

Equation of thermal conductivity:

$$C_i(T)\frac{\partial T(x,y,\tau)}{\partial\tau}=\frac{1}{x}\frac{\partial}{\partial x}\left(x\cdot\lambda_{x,i}(T)\frac{\partial T(x,y,\tau)}{\partial x}\right)+ \\ +\frac{\partial}{\partial y}\left(\lambda_{y,i}(T)\frac{\partial T(x,y,\tau)}{\partial y}\right)+q_V(x,y,\tau), \qquad (1)$$

$$(x,y)\in\Omega,\ \ \tau\in\left]0,\tau_m\right],\ \ i=\overline{1,N};$$

$$\tau=0 \qquad T(x,y,0)=T_0(x,y); \qquad (2)$$

$$\partial\Omega_1\cap\partial\Omega \qquad T(\partial\Omega_1,\tau)=T_w(\partial\Omega_1,\tau); \qquad (3)$$

$$-\lambda_i(T)\frac{\partial T(\partial\Omega_2,\tau)}{\partial n}=A_i(T)q_w(\tau)-$$

$$\partial\Omega_2\cap\partial\Omega \qquad -\varepsilon_i(T)\sigma_0\left(T^4(\partial\Omega_2,\tau)-T_f^4\right)- \qquad (4)$$

$$-h_f(T)(T(\partial\Omega_2,\tau)-T_f).$$

Equation of radiative heat transfer (diffusion approximation):

$$\frac{1}{x}\frac{\partial}{\partial x}\left(x\cdot D_{x_i,\nu}(T)\frac{dU_\nu(x,y)}{dx}\right)+\frac{\partial}{\partial y}\left(D_{y_i,\nu}(T)\frac{dU_\nu(x,y)}{dy}\right)- \tag{5}$$

$$-k_{i,\nu}(T)\cdot U_\nu(x,y)=-k_{i,\nu}(T)\cdot B_\nu^*(x,y,T);$$

$$(x,y)\in\Omega,\quad i=\overline{1,N}$$

$$\begin{aligned}&-\frac{3}{2}D_{i,\nu}(T)\left(\frac{1}{3}+\tilde{R}_{11,\nu}\right)\frac{dU_\nu(\partial\Omega_3)}{dn}+\\ \partial\Omega_3\cap\partial\Omega\quad &+\frac{1}{2}\left(\frac{1}{2}-\tilde{R}_{01,\nu}\right)U_\nu(\partial\Omega_3)=\\ &=q_{W,\nu}(\partial\Omega_3,\tau)(2\eta_{W1}^{d}\tilde{Q}_{01,\nu}+\eta_{W1}^{\delta}\tilde{Q}_{1,\nu});\end{aligned} \tag{6}$$

$$\begin{aligned}&-\frac{3}{2}D_{i,\nu}(T)\left(\frac{1}{3}+\tilde{R}_{11,\nu}\right)\frac{dU_\nu(\partial\Omega_4)}{dn}+\\ \partial\Omega_4\cap\partial\Omega\quad &+\frac{1}{2}\left(\frac{1}{2}-\tilde{R}_{01,\nu}\right)U_\nu(\partial\Omega_4)=\\ &=2\cdot\tilde{E}_{1\nu}n_{i,\nu}^2(T)\cdot B_\nu(\partial\Omega_4,T),\end{aligned} \tag{7}$$

where $q_V=\int\limits_{\nu}k_{i,\nu}(T)\cdot\left(U_\nu(x,y,\tau)-B_\nu^*(x,y,T)\right)d\nu;$

$U_\nu=\int\limits_{0}^{4\pi}I_{i,\nu}(x,y,\omega)d\omega,\ B_\nu^*(x,y,T)=4n_\nu^{\ 2}(T)\cdot B_\nu(x,y,T).$

In (5)-(7) $\partial\Omega_3$ – part of the border which is semi-transparent for external radiation; $\partial\Omega_4$ – part of the border which is opaque for external radiation.

Extreme statement of IP and the iterative regularization method solving was used:

$$S(\vec{u})=\frac{1}{2}\int_0^{\tau_m}\sum_{n=1}^{N_t}\left(T\left(x_n^t,y_n^t,\tau\right)-T^e\left(x_n^t,y_n^t,\tau\right)\right)^2 d\tau;$$

$$\vec{u}=\left\{\lambda_y\left(T\right),\lambda_x\left(T\right)\right\}, \tag{8}$$

where τ_m – duration of the experiment; N_t points temperature is measured.

Condition of the cessation of the iteration process of functional minimization:

$$S(\vec{u})=\min;\ S\geq\Delta^2,$$

where Δ – summarized error of temperature calculations and measurements.

To transform minimization procedure (8) into a finite-dimensional form, parameterization of required temperature dependences is conducted:

$$\lambda_x(T) = \sum_{i=1}^{K_{\lambda x}} \lambda_{xi} \chi_{1i}(T); \quad \lambda_y(T) = \sum_{j=1}^{K_{\lambda y}} \lambda_{yj} \chi_{2j}(T), \qquad (9)$$

where χ_{1i}, χ_{2i} – basis functions.

Simulations of thermal tests conditions

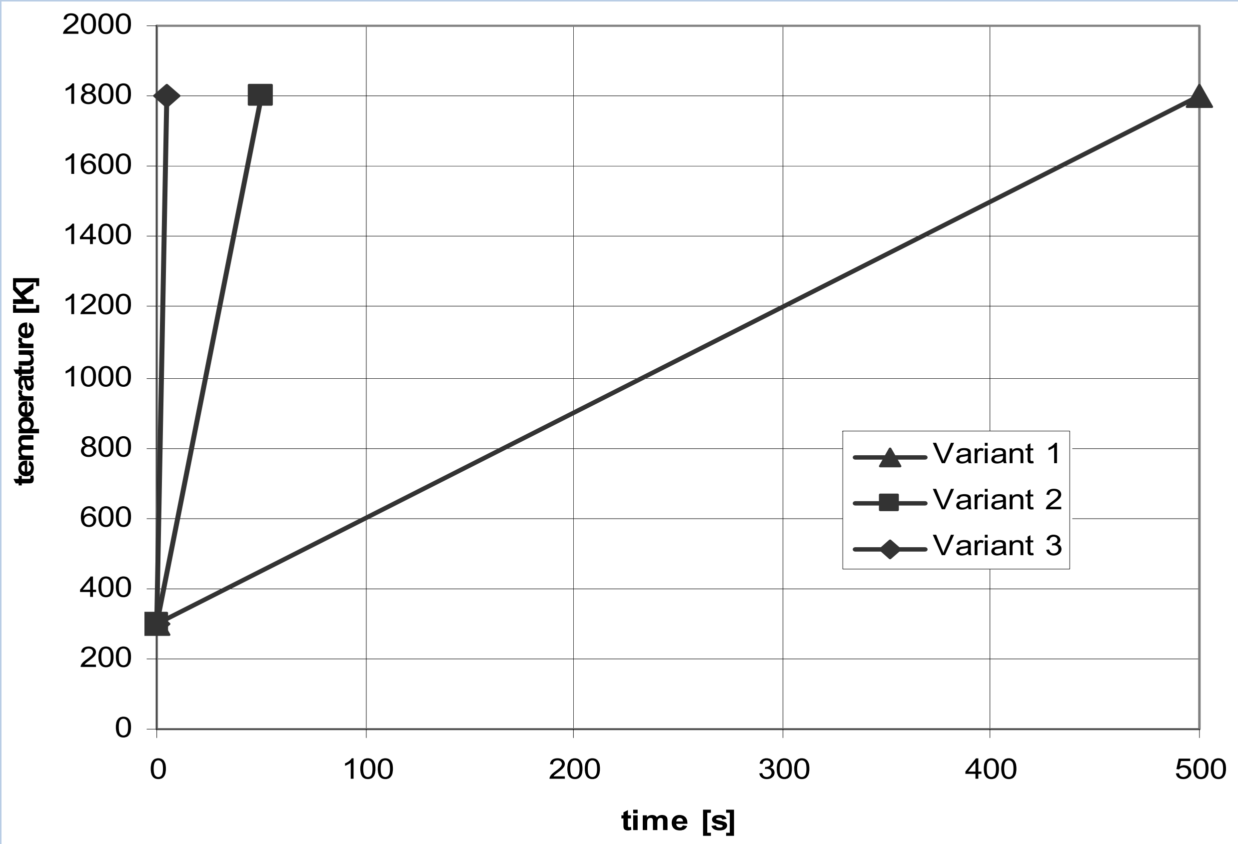

Variants of temperature dependences of the frontal surface from duration

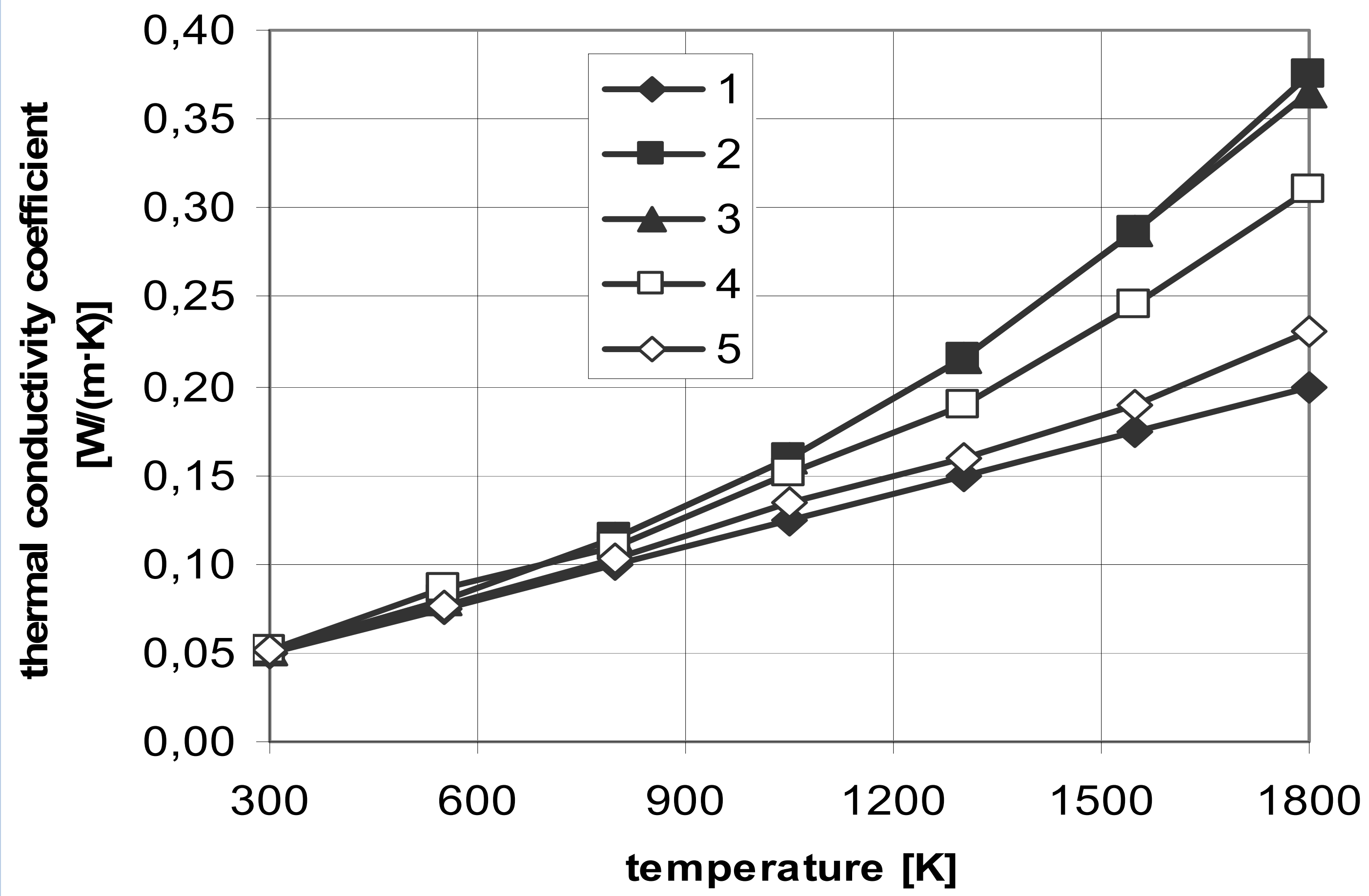

Thermal conductivity coefficients for semitransparent porous material: 1 – λ; 2 – λ_{ef} as per Rosseland; 3 – λ_{ef} values in case of changes of frontal surface temperature as per variant 1;4 –same for variant 2; 5 –same for variant 3

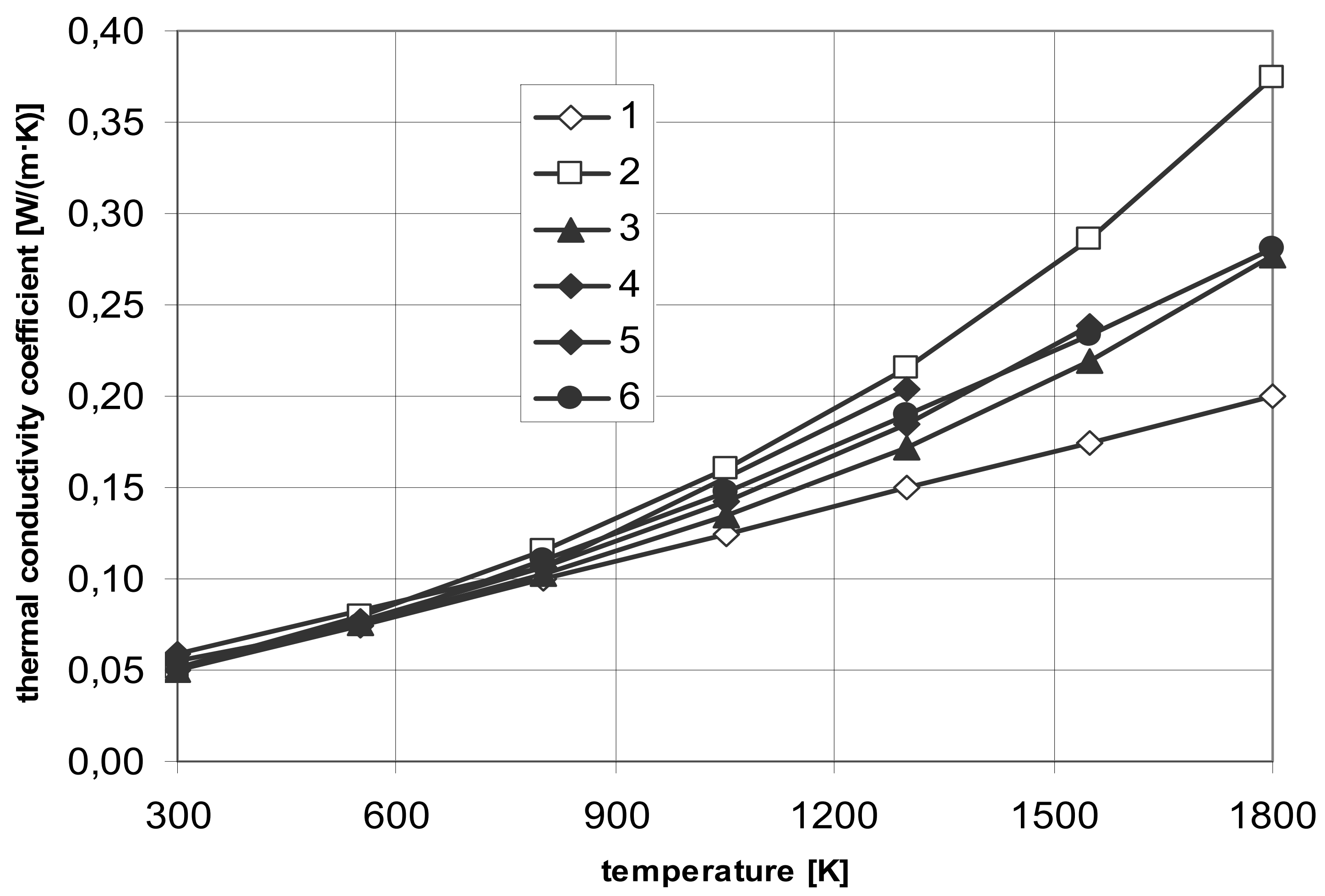

Thermal conductivity coefficients for semitransparent porous material: 1 – λ; 2 – λ_{ef} as per Rosseland; 3 – λ_{ef} value using thermocouple indication values at the depth of 1 mm; 4 – same for 3 mm; 5 – same for 5 mm; 6 – same in case of all three sensors

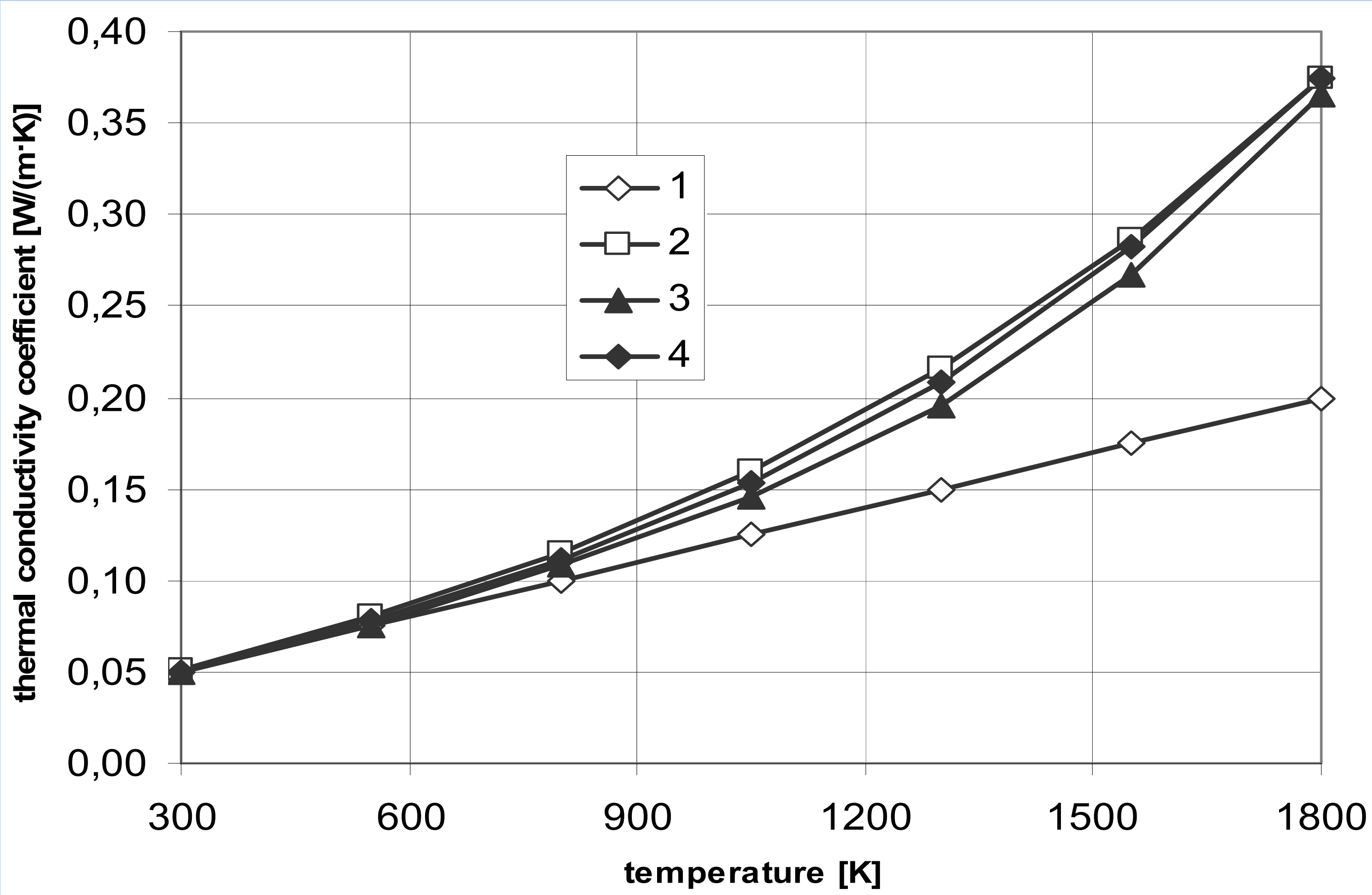

Thermal conductivity coefficients for semitransparent porous material: 1 – λ; 2 – λ_{ef} as per Rosseland; 3 – λ_{ef} value using thermocouple indication values at the depth of 1 mm; 4 – same for 5 mm

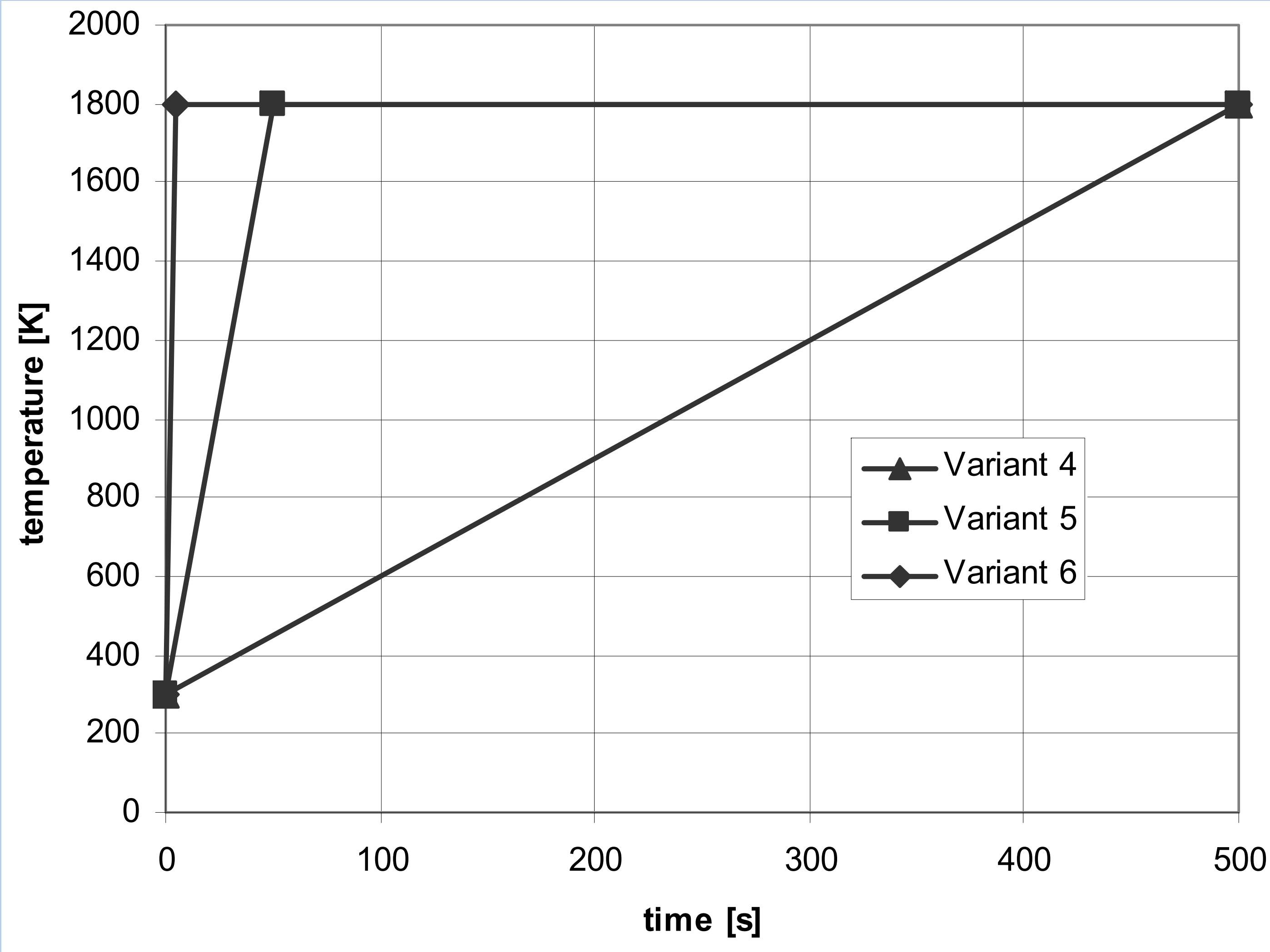

Variants of temperature dependences of the frontal surface from duration

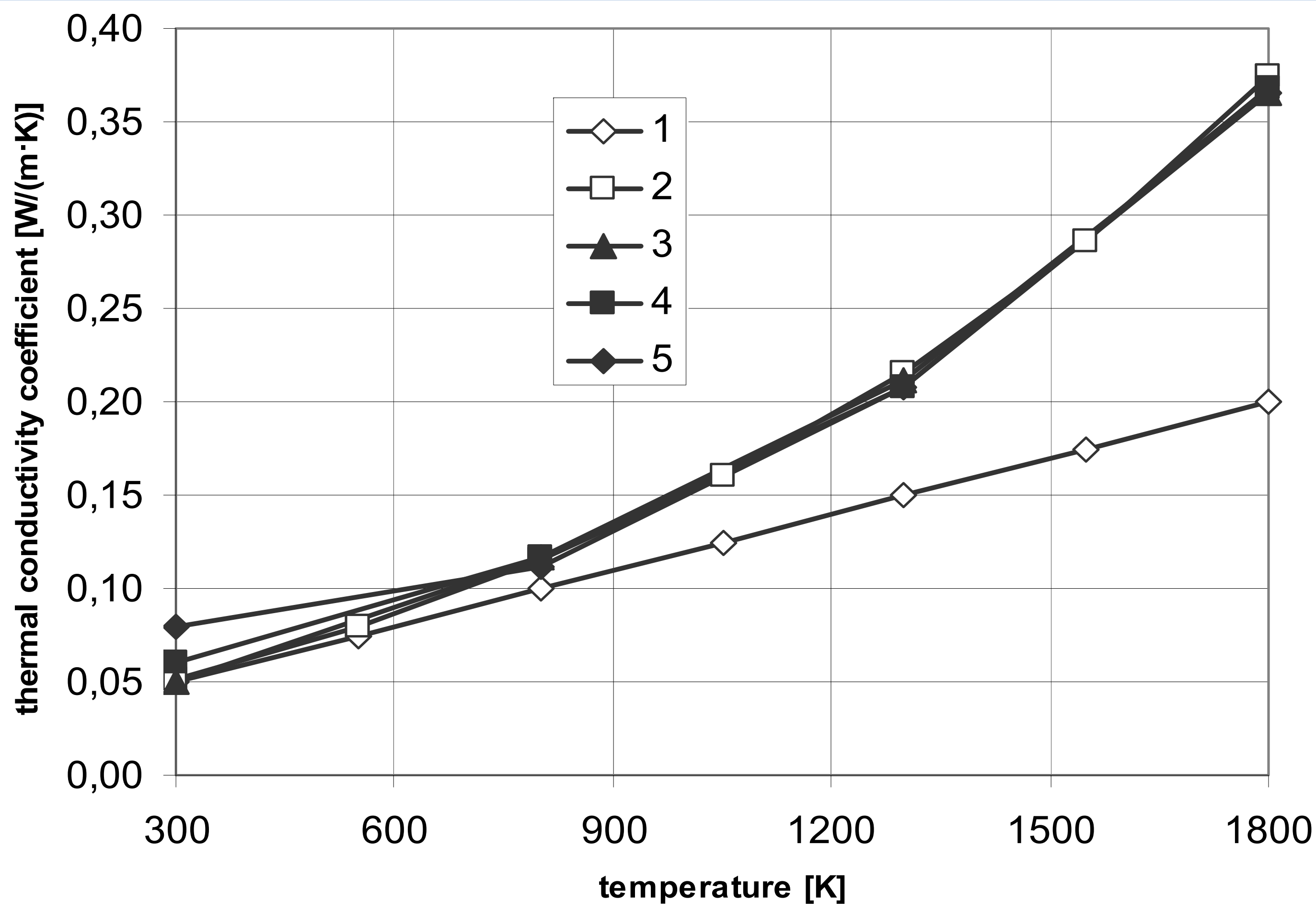

Thermal conductivity coefficients for semitransparent porous material: 1 – λ; 2 – λ_{ef} as per Rosseland; 3 – λ_{ef} values in case of changes of frontal surface temperature as per variant 4; 4 –same for variant 5; 5 –same for variant 6

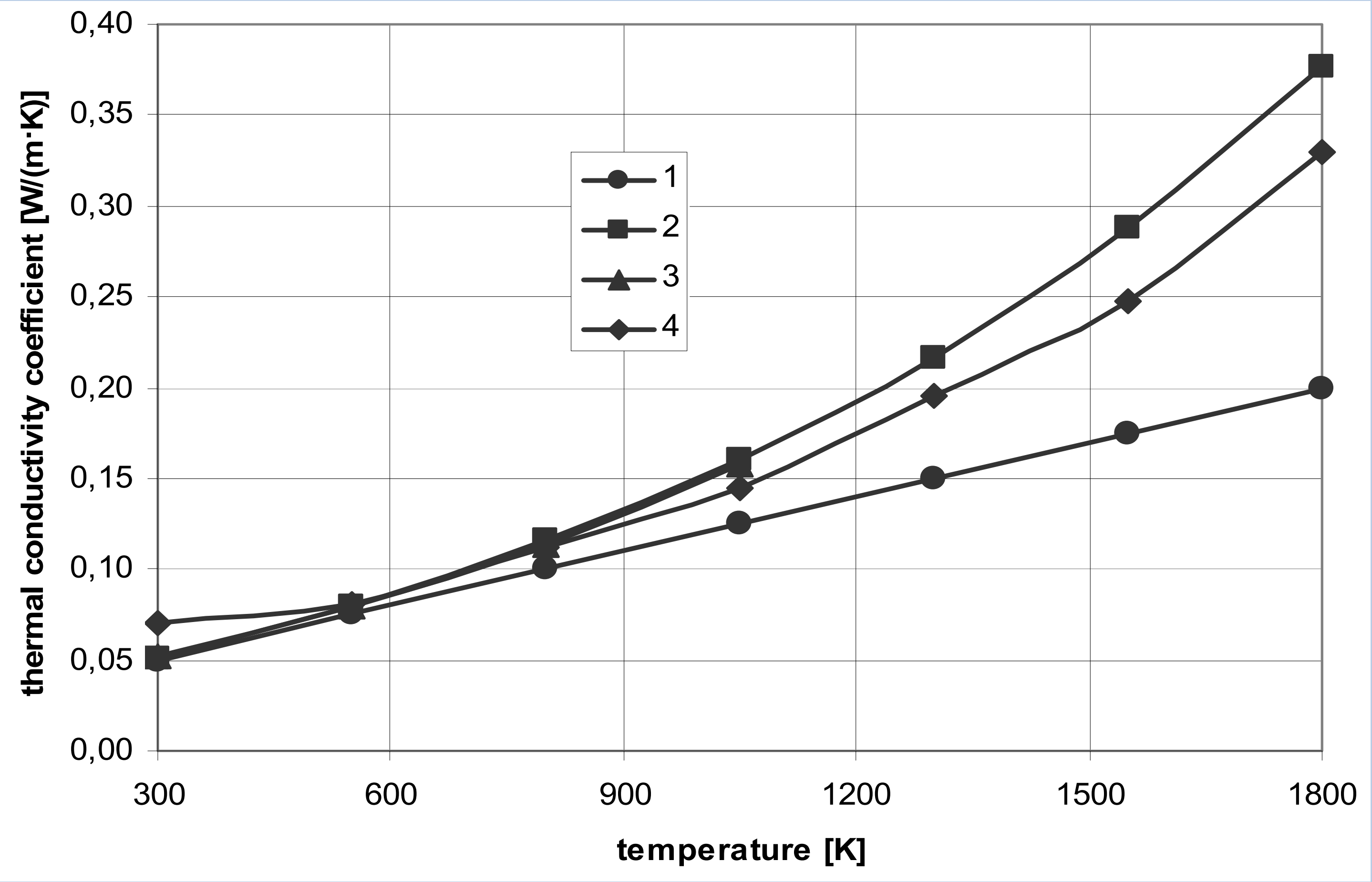

Thermal conductivity coefficients for semitransparent porous material: 1 – λ; 2 – λ_{ef} as per Rosseland; 3 – λ_{ef} values in regime of heating with radiation flux is $0.25 \cdot 10^6$ W/m^2; 4 – same for $1.5 \cdot 10^6$ W/m^2

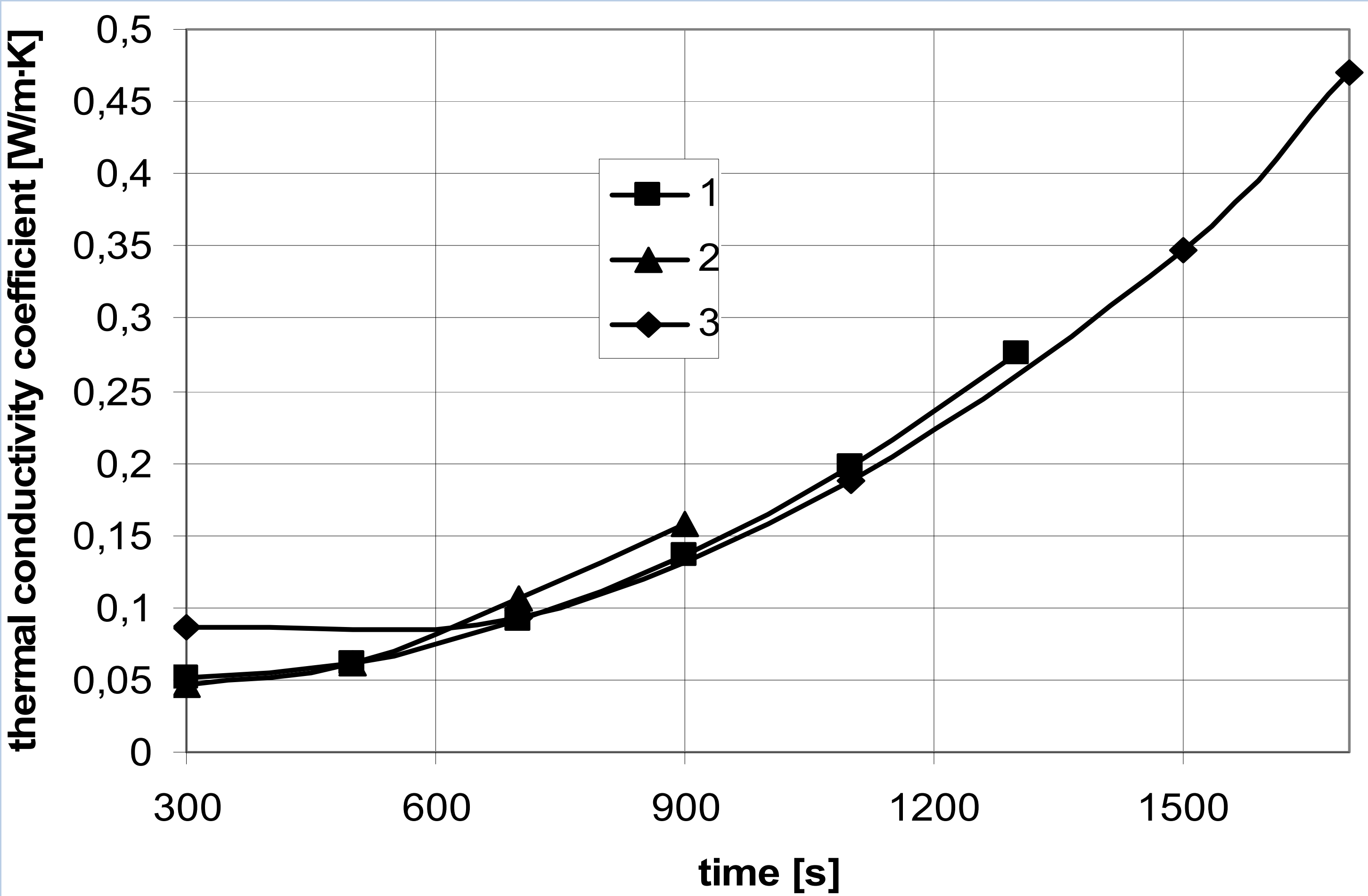

Effective thermal conductivity coefficients for semitransparent porous material:
1 – radiation flux density is $0.18 \cdot 10^6$ W/m^2; 2 – $0.37 \cdot 10^6$ W/m^2; 3 – $1.2 \cdot 10^6$ W/m^2

Thank you for your attention